October 2014

Application of Satellite Data to Model Storm Runoff Into Rosamond Dry Lake

Mridul Oli
Loyola Marymount University, oli.mridul@gmail.com

Application of Satellite Data to Model Storm Runoff Into Rosamond Dry

Lake

by

Mridul Oli

A thesis paper presented to the

Faculty of the Department of

Environmental Science and Civil Engineering

Loyola Marymount University

In partial fulfillment of the

Requirements for the Degree

Master of Science in Environmental Science

We are submitting herewith a thesis written by Mridul Oli entitled "Developing a Model to Calculate Runoff into Rosamond Lake". We have examined the final electronic copy of this thesis for form and content and recommend that it be accepted in partial fulfillment of the requirements for the degree of Master of Science in Environmental Science.

_____

Jeremy S. Pal, Thesis Advisor

_____

Jose A. Saez, Thesis Advisors

We have reviewed this thesis and recommend its acceptance:

_____

Victor Carmona, Thesis Committee Member

_____

Brian Dietrick, Thesis Committee Member

Acknowledgements

Abstract

Antelope Valley is situated in Southern California and is bounded by the Tehachapi and the San Gabriel Mountains. It stretches over 2,200 mi^2 and encompasses Rosamond Dry Lake and the 1,200 mi^2 watershed draining into it. The cities of Lancaster and Palmdale are the two major urban centers that lie in the watershed draining into Rosamond Dry Lake. The lake lies within the vicinity of the Edwards Air Force Base and provides an important site for aviation research and test operations in addition to ecosystem services. Hence, it is necessary to balance the need to remove water from the lake to support Edwards Air Force Base's aircraft missions and the need to inundate the lake to protect the its surface and the ecosystem it supports.

In this study, satellite-based elevation, state of the science land cover and soil data are used to create a model that predicts storm runoff volume into Rosamond Dry Lake. Geographical Information Systems software is used delineate and divide the watershed into 98 sub-basins. Each sub-basin is assigned a land cover type, percent impervious area, and hydrologic soil type to calculate the Natural Resource Conservation Service curve number. The model also incorporates two detention basins to represent existing flood control structures in Lancaster and Palmdale. Runoff in each subbasin is estimated using the Natural Resource Conservation Service Curve Number method and accumulated into the channels.

In a hydraulic modeling software developed by the Army Corps of Engineers, the modeling system is applied to calculate the total storm runoff volume into Rosamond Dry Lake for ten historical storm events as well as a 100-year event. Due to the lack of stream gauge data, a technique that couples Landsat 7 satellite images of Rosamond Lake with LIDAR elevation data to estimate observed runoff volume is developed to evaluate model performance. In comparison to these estimates, the model overestimates runoff volume by approximately 7%. However, there are considerable biases for two storm events that are caused by the effects of evaporation, wind and snow on the lake's water and various deficiencies in the model.

The impacts of past and future urbanization on the runoff volume into the lake are examined by modifying the curve number in sub-basins representative of the urban centers. For a 100-year, 24-hour, precipitation event, urbanization results in increased runoff at both the sub-basin and watershed levels. Additional simulations indicate that measures such as building detention basins and repurposing unused or undeveloped areas within an otherwise developed area (infill) can mitigate increased runoff due to urbanization.

Overall, the model proves to be an effective tool for predicting runoff into Rosamond Dry Lake. It can also be used to study the rainfall-runoff processes in the lake. The ability to predict water volumes in the lake will allow engineers and planners to establish a balance between the Air Force Base's aircraft missions and the lake's ecological function. Lastly, the techniques used to develop the model can be used to develop similar models for other watersheds.

Contents

List of Figures and Graphs

Equations

- Equation 1: Relationship between runoff and rainfall for the curve number method.
- Equation 2: Relationship between runoff curve number and soil retention.
- Equation 3: Relationship between soil retention and initial abstractions.
- Equation 4: Equation for the calculation of basin lag time.
- Equation 5: The elevation-based, 100-year, 24-hour, storm relationship developed in FMD04.
- Equation 6: Equation for the calculation of climatic index.
- Equation 7: Storage calculation for Muskingum Routing.

Tables

- Table 1: Historical climate data for the RDL watershed. These values are derived from 11 USGS stations with data collection period ranging from 5 years to 100 or more years (North State Resources, 2010).
- Table 2: Antecedent Moisture Condition (AMC) classification based on total accumulated precipitation according to the National Engineering Handbook, Section 4 (1972).
- Table 3: Categorization of AMC based on cumulative precipitation values (0.04 in is subtracted for days with no rain) of the previous day.
- Table 4: Runoff comparison for ChanLoss_FM. Of the three sets of values for FTLC, 61% is used in the FM..
- Table 5: List of simulations carried out in this study. Precipitation implies the type of precipitation data used for the simulation, while flood control implies the presence or absence of detention basins in the city of Lancaster and Palmdale. Simulations performed on the simplified model end with the suffix "SM" while all simulations performed on the full model end with "FM".
- Table 6: Comparison of key hydrological parameters in FR04 and SM. Since the sub-basins are categorized based on elevation ranges, average values for lowest and highest elevation are mentioned.
- Table 7: Range of Hydrological Parameters in the Full Model.
- Table 8: Runoff volume estimation based on Landsat images. Columns 1 and 2 are the dates when the images were taken. Column 3 is the average wind speed on the day when the post-storm image was taken and 4 is the wind temperature in RDL during the period between the pre-storm image and post-storm image. Column 5 is the cumulative precipitation during that time while column 6 is the lag between the end of the storm and the final Landsat image date, 2. And finally, column 7 is the runoff caused by the event.
- Table 9: Runoff comparison between the FM in present conditions and FM with the detention basins removed (NoDet_FM).
- Table 10: Table of variables and runoff for FM and NoUrbn_FM_P100. Note that the manipulated sub-basins are highlighted in blue.

Chapter 1: Introduction

Located in the Antelope Valley and within the boundaries of Edwards Air Force Base (EAFB), Rosamond Dry Lake (RDL) is a playa that spans approximately 22 mi^2. EFAB uses the lake for aviation research and test operations (Deal, 2013). And, the National Aeronautics and Space Administration's (NASA) Dryden Flight Research Center has used the playa as a landing site for operational flights and space shuttle tests since 1977 (EAFB Public Affairs, 2006; Dunbar, 2008). There are, however, several challenges in using RDL for the aforementioned purposes.

When RDL is inundated, the surface cannot be used for aircraft takeoff and landing. Furthermore, Rosamond Boulevard, one of the three entrances to EAFB, becomes unusable (French et al., 2006). The presence of water is conducive of life as it attracts several desert and migratory animal species. The presence of birds in the vicinity of the lake poses a safety hazard to the air-force pilots.

Removing water from the lake completely to meet the needs of EAFB aircraft mission is disadvantageous. Lack of water in the lake is detrimental for the desert ecosystem. Furthermore, extended dry periods cause the clay on the normally flat and smooth lakebed to dry and crack. And dust emitted from the dry surface enters jet engine intakes and hinders pilots' vision (Experimental Aircraft Association, 2010). Lastly, arid conditions leave the lakebed susceptible to wind erosion that eventually leads to dust storms.

Dust storms negatively impact human health and degrade the environment. For instance, dust on snow makes it darker causing it to absorb more solar radiation (sunlight) and melt faster (Harris, 2006). Moreover, Antelope Valley Resource Conservation District's (AVRCD) website states that dust storms also damage buildings. Anecdotal and video evidence show buildings in the Mojave Desert fully covered in dust.

It is necessary to balance the need to remove water from RDL to support EAFB's aircraft missions and the need to inundate it to protect the lake's surface and the ecosystem it supports. As such, EAFB and other stakeholders in the region have an interest in determining the amount of water that accumulates in the lake to establish a balance among EAFB's aircraft missions while continuing to preserve and restore natural habitats as well as maintain the lakes' surface (Deal and IRWM, 2013).

A viable solution to the competing needs of EAFB aircraft mission and the preservation of natural system is to implement controlled seasonal discharges into the RDL. EAFB and the Los Angeles

County Sanitation Districts (LASCD) currently coordinate controlled discharges of tertiary-treated water from the Lancaster Water Reclamation Plant (LWRP) into Piute Ponds which occasionally overflows into RDL. An improved understanding of the runoff into RDL would enable EAFB to fulfill their mission while protecting the local habitats and managing LWRP's excess runoff. Moreover, periodic flooding of the lake is necessary to maintain the smooth surface of the runway (Deal, 2013). After all, it is the movement of surface water that results in a flat and smooth playa surface.

The intent of this thesis is to develop a spatially distributed rainfall-runoff model of the watersheds contributing to RDL that calculates runoff volume in the lake and tests the following hypotheses:

- The curve number approach coupled with satellite data is effective in estimating runoff.
- Past urbanization in desert regions has increased runoff.
- In cities, infill generates less additional runoff than sprawl.

This document is divided into five sections including this introduction as Chapter 1. Chapter 2 provides a review of relevant literature. Chapter 3 contains descriptions of the software, datasets, methods and model parameters. This is followed by a presentation of the results in Chapter 4. Conclusions and future recommendations are provided in Chapter 5. An appendix containing detailed tables, glossary of terms and information regarding data manipulation and processes is also provided.

Chapter 2: Literature review

2.1 Playas

Playas, Spanish for beaches, are flat-bottomed dry lakes that form ephemeral shallow wetlands. They are common in arid and semi-arid environments and the highest density of playas is found in the Great Plains (Smith, 2003). Customarily, playas are the lowest point of a watershed. It is conjectured that playas are evinced by wind action or subsidence of land (United States Environmental Protection Agency (US-EPA), 2012). Most playas have a slope of less than 0.0002 and are one of the flattest landforms (Baker, 1988).

The availability of groundwater discharge (water discharged from the water table to the surface due to its proximity to the water table) determines the nature of a playa surface (Motts et al., 1969). Most playa soils have high clay content since coarser materials tend to be deposited upstream and only fine-grained materials collect at the playa. Soils found in playas are typically hydric (Smith, 2003) (saturated with water and tend to be anaerobic as they are formed under saturated conditions (Natural Resource Conservation Service)). At the center of the playa, the soil clay content frequently exceeds 80% while it is much lower (50%) in the edges. Because they are the lowest point of the watershed, playas are receptors of sediments in the form of dust, salts and minerals (Baker, 1988). The concentrations of these sediments in conjunction with groundwater, when present, determine the properties of a playa's surface (Baker, 1988). Over time, the accumulation of these sediments form an inconspicuous, microbial organism-held, crust over the surface of the playa (Motts et al., 1969; Brostoff, 2001). The crust is critical for the ecological functions of the playa; it support the survival of desert animals, influences the existence of desert flowering plants and assist the symbiosis of soil particles with algae and fungi (Brostoff, 2001).

Since playas exist in arid conditions where evaporation exceeds precipitation, they are ephemeral lakes capable of supporting an ecosystem at certain times of the year and a clayey depression in the middle of a vast desert otherwise (Baker, 1988). The main source of water in playas is precipitation and storm runoff. In some cases, groundwater discharge from underlying aquifers also contributes (Baker, 1988). Playas are covered with water for less than three months each year (Neal, 1975). However, depending on the frequency and magnitude of precipitation, playas can stay ponded in consecutive years or not pond an entire year (Cooke et al., 1993). The flatness of playas and the impermeability of clay render a landscape that is susceptible to inundation. Even a small storm event can inundate a large

surface area, which makes it difficult to predict flood hazard (French et al., 2006). Most of the water in playas is lost through evaporation, however, there is some transpiration, when vegetation is present, absorption and infiltration (Smith, 2003; Neal, 1965). Runoff also enters the water table through the cracks formed in a playas surface during a dry spell.

In addition to being hydrologically significant, playas are also important to the surrounding ecosystem. Because of their frequently fluctuating wet-dry cycle, they are able to support a variety of plants and animals. According to the US EPA (2012) two million waterfowl migrate to playas in the Southern White Plains during the winter months. It is believed that playas, collectively, support some 235 animal species and 350 plant species (Smith, 2003). The US EPA (2012) attributes the presence of amphibians in arid reasons on the existence of playas.

Several anthropogenic activities threaten the well-being of playas (US EPA, 2012). Firstly, higher temperatures resulting from anthropogenic climate change tend to induce higher evaporation rates and reduce infiltration and soil moisture. Secondly, anthropologically-accelerated sedimentation increases the concentration of sediment clog, and reduces infiltration and soil moisture (Bartuszevige et al., 2012). Thirdly, dry farming and new irrigation techniques reduce runoff into the playa through the diversion of water for agriculture (US EPA, 2012). In addition, dumping human and animal waste into playas compromises water quality and poses a threat to wildlife (US EPA, 2012). Lastly, many playas serve as an important location for military interests. Most air-to-ground shooting ranges in the United States operate around playas in California, Nevada, Arizona, Utah and New Mexico (Underwood and Guth, 1998). Furthermore, the naturally flat surface of playas provide ideal natural runways for flying as well as testing aeronautics. The use of playas for these purposes is known to damage their soil crust.

2.2 Rosamond Dry Lake

RDL is a playa located in the Antelope Valley, Mojave Desert. Antelope Valley is bounded on the north by the Tehachapi Mountains and the south by the San Gabriel Mountains (Figure 1). Storm runoff from three sub- watersheds, Amargosa Creek, Cottonwood Creek and Littlerock Creek, which together comprise and area of approximately 1,200 mi^2, flows into RDL (U.S. Army Corps of Engineers (US ACE), 2010). RDL is the lowest point in the watershed at 2275 ft, while the highest point is 8250 ft at the ridges of the San Gabriel Mountains. Consequently, the watershed varies from high desert in lowlands and forest with snow in the mountain. The cities of Lancaster and Palmdale and Rosamond town lie within the boundaries of the watershed.

4
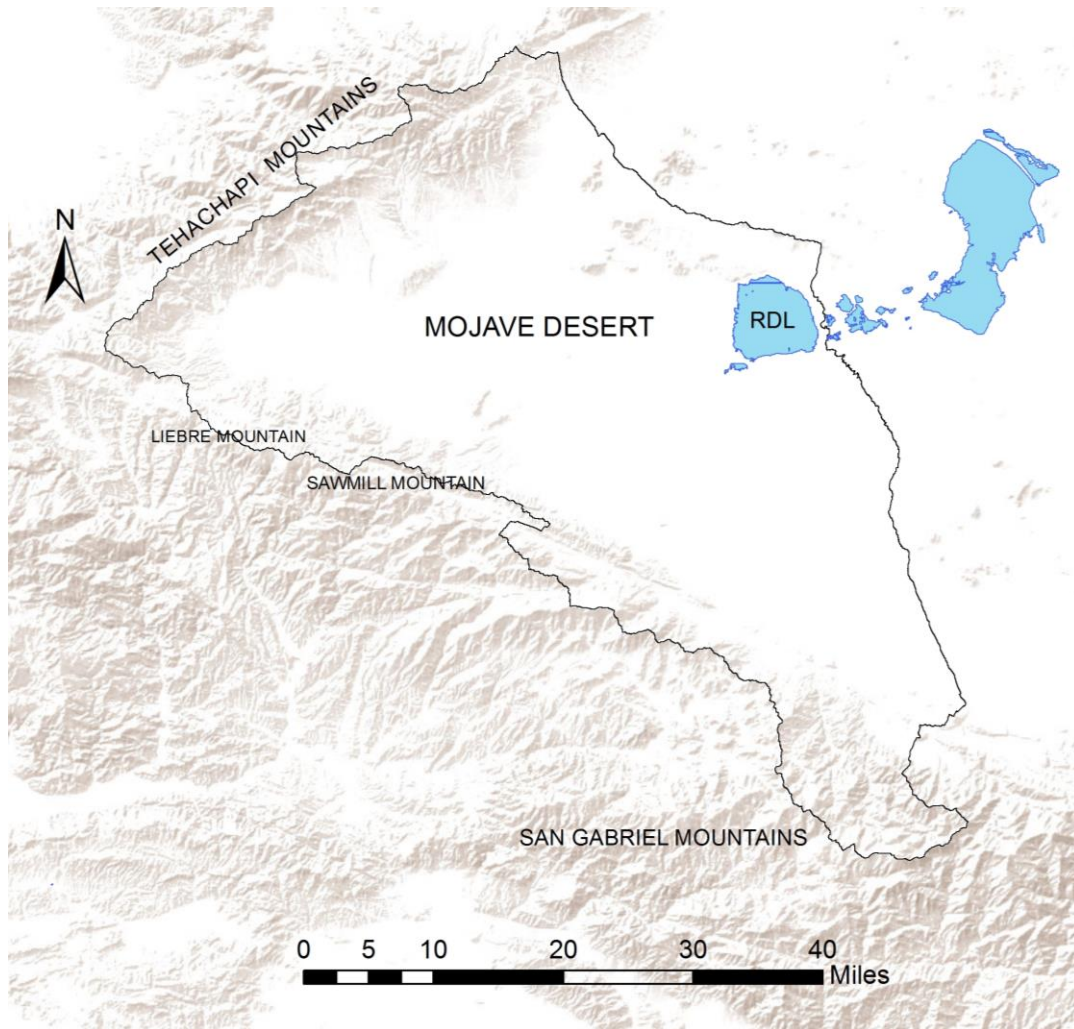
Figure 1: Terrain map of the watershed showing the location of major mountains.

As is typical of Southern California, the watershed experiences a Mediterranean climate with long summers and short winters. The climate varies with elevation (Table 1). The average annual temperature ranges from 44°F to 77°F; the median annual precipitation ranges from 5.5 in to 13.7 in; and the mean annual snowfall from 1.6 in to 16.1 in with most of the snow falling 4000 ft above mean sea level (amsl) (North State Resources, 2010). Approximately 80% of the rainfall occurs in the winter, between the months of November and March (Brostoff, 2001). Although most of the precipitation is caused by low-intensity and long-duration frontal storms originating in the Pacific Ocean, some portion of the precipitation is caused by high-intensity and low-duration flash storms during the summer months. (North State Resources, 2010).

Table 1: Historical climate data for the RDL watershed. These values are derived from 11 USGS stations with data collection period ranging from 5 years to 100 or more years (North State Resources, 2010).

Elevation (ft amsl)	Number of Stations	Annual Average Temperature (°F)		Annual Precipitation (in)		Annual Snowfall (in)
		Minimum	Maximum	Median	High	Mean
below 3070	9	44	77	5.5	36.6	1.6
above 4000	2	47	77	13.7	41.0	16.1

       RDL is about 100 mi northeast of Los Angeles (Dunbar, 2008) and stretches over an area of 22 mi^2. With an approximate diameter 6 mi, RDL's range of elevation is less than 18 in (EAFB Public Affairs, 2006). Motts et al. (1969) classify the lake as a fine-grained playa. The lake surface's morphology changes frequently depending on groundwater discharge, temperature, nature of rainfall and associated runoff (Motts et al., 1969). Since, there is no outlet to any other water body (ocean or river), the lake is also often called a terminal lake. The extremely flat and shallow lakebed's predominant component is clay. Clays do not infiltrate well, but retain any water that does infiltrate. As a result, clay soils have a high water content, but are poor hydraulic conductors (USGS, 2001); they are also known to swell when wet and shrink and crack when dry (Figure 2). Due the lakebed's flat topography, a relatively small volume of water can inundate a considerable surface area of the lake. In addition, the water body's movement is unpredictable and susceptible to changes in wind intensity and direction. The dominant mechanism for water leaving RDL is through evaporation. Although a majority of the lake's surface is hard and smooth, a tiny fraction, close to the groundwater table, is soft (Dutcher and Worts, 1963). Infiltration mostly occurs in these soft areas (Dutcher and Worts, 1963). With no outlet and low permeability within the lakebed, inundation duration, mainly governed by the rate of evaporation, is unpredictable.

Figure 2: An image of the surface of RDL. Because of the high clay content, the soil shrinks and cracks if left dehydrated for an extended period.

The sediments that lie on the lake's surface are remnants of the deposits in Lake Thompson, a water body which occupied most of Antelope Valley during the Pleistocene era, 2.6 million to 11,700 years ago (Motts et al., 1969). More than half of RDL's surface is covered by crypto-biotic crusts – a mixture of soil and microbes (Bronstoff, 2001). However, the crust discontinues with depth (Motts et al., 1969). The veneer of crypto-biotic crusts on the surface of RDL serves three main functions:

- It seals the surface of the lake. This prevents the erosion of soil and consequent sandstorms by trapping the dust from the dry soil (Goudie, 1978). On the other hand, it also inhibits precipitation from directly entering the water table through cracks formed in the soil.
- It serves important ecological roles such as carbon fixation, nitrogen fixation, energy absorption, seed germination etc. (USGS, 2001).
- It helps sustain the desert ecosystem and organisms, such as brine shrimp eggs, which are known to be stored in biological crusts (Gwynn, 2006; Chandler, 1991).

In the past, Rosamond Lake ponded perennially (EAFB Public Affairs, 2006). Based on Landsat images and archived precipitation data from 1942 to 2001, Lichvar et al. (2004) concluded that the ponding frequency of RDL is 0.51 (every other year). An examination of the Landsat satellite images of the lake show that, between 2001 and 2011, RDL has ponded every year. When inundated, at least four

7

different species of desert shrimp species are found in the lake (Chandler, 1991). The presence of brine shrimp causes an influx of birds into the lake and surrounding areas. The lake serves as a feeding site as well as a stop for migratory birds (Chandler 1991). Some endangered species of flora and fauna, like desert turtles and Rosamond eriastrum, are also found in RDL (California Native Plant Society Inventory Plant Detail, n.d.). Lastly, the lake has been used by the military also.

Rosamond and Rogers Lake lie entirely within the boundaries of EAFB. The military's use of the lakebeds dates back to the 1930's when they were used by the Army Air Corps for target practice (NASA, n.d.). The two lakes were activated in 1951 and have been used as landing sites for operational flights since 1977 (EAFB Public Affairs, 2006). In the past, NASA Dryden Flight Research Center has used RDL's surface as a landing strip for space shuttles and test flights (Dunbar, 2008). Furthermore, Rosamond Boulevard, one of three access routes to EAFB, runs across RDL (French et al., 2006). Water in the lake causes various administrative and logistic issues for EAFB and other stakeholders. Of particular importance is the elevated likelihood of Bird Air Strike Hazard (BASH) as training planes that frequently fly in the area have windshields that are unable to deflect birds (Morland, 2007). An estimated 500 bird-aircraft collisions occur annually in military bases across the United States (Myers, 1992) and since 1972, no less than 33 pilots have lost their lives due to such collisions (Thompson, 2013). However, as stated earlier, having water in the lake is also beneficial for the ecosystem and lake surface.

2.3 Urbanization and Rosamond Lake

Rosamond Lake and the water flowing into it have endured the impacts of urbanization. To counter the increased runoff caused by land-development in Antelope Valley, LACSD, District 14, used the natural drainage provided by Amargosa Creek to dispose the city of Lancaster's treated wastewater into RDL (Friends of Piute Ponds, n.d.). Then, a dike was built to cope with the consequent flooding, thus, engendering the development of the Piute Ponds (Friends of Piute Ponds, n.d.).

Piute Ponds, man-made surface water dams and detention basins in the RDL watershed, have reduced storm runoff that collects in RDL. They lie within the boundaries of EAFB and stretch over 400-acres (Figure 3). These interconnected ponds were constructed in 1961 to manage effluent, tertiary-treated water, from the Lancaster Water Reclamation Plant (LWRP) (Environmental Science Associates (ESA), 2004). When there is minimal demand for LARWP's reclaimed water, the ponds get filled beyond capacity and water overflows into RDL (Alderman et al., 2009). The discharge, which reaches several

million gallons per day, varies seasonally based on an agreement between EAFB and LACSD. This agreement helps maintain at least 200 acres of wetland habitat (LACSD, n.d.).

Figure 3: The several ponds that constitute Piute Ponds. Source: Google Maps, 2014.

Ducks Unlimited, a nonprofit organization of duck hunters that also works for the conservation of waterfowl and wetland, has been developing and renovating Piute Ponds. The organization has installed new water control structures in Piute Ponds which has enabled the utilization of areas (Ducks Unlimited Pond) that were left unused for years (Friends of Piute Ponds, n.d.). The organization also plans on renovating Little Piute in the near future.

2.4 Importance of Flood Modeling in Rosamond Dry Lake

Water from LWRP is primarily used for agricultural and landscaping purposes. Hence, there is a minimal demand for LWRP's water from late fall to early spring (Alderman et al., 2009). It is during this period when excess treated water from the LWRP flows into Piute Ponds and sometimes overflows into RDL (Alderman et al., 2009). Incidentally, overflows into RDL are highest at the time of the year when the rate of evaporation is low (Alderman et al., 2009) and there is a higher likelihood of precipitation.

RDL is a natural sink. Hence, runoff from the watershed eventually finds its way to the lake. Changes in runoff volume into RDL is susceptible to land development and urbanization. While deforestation and construction projects increase runoff, construction of flood control structures and transforming deserts into agricultural land decreases runoff. A central goal of this study is to develop a model that estimates runoff volumes into RDL. A model would aid the study of the implications of precipitation and inundation levels in RDL. This is imperative to balance EAFB's mission with RDL's ecological function while preserving and maintaining its surface.

2.5 Pertinent Studies and Technical Manuals

GIS applications have been implemented for water resource engineering for quite some time. Tauer and Hamborg (1992) use GIS to identify sites for developing irrigation systems in Mali. Stuebe and Johnston (1990) calculate runoff for six different watersheds analytically and using GIS to conclude that GIS surpasses the limitations of conventional methods. French et al. (2005) use GIS to estimate the 100-year regulatory flood depth in Rogers and Rich Dry Lake in California. French et al. (2006) also examine satellite images of Rosamond Dry Lake to verify the use of the NRCS curve number approach in their study. Yuan (2007) uses GIS to analyze the impacts of land-cover change on various aspects of the Greater Mankato Area of Minnesota including storm runoff and water quality. Of the numerous GIS-based hydrologic research, the works of French et al. (2004, 2006) on Rosamond Dry Lake are particularly relevant to this study.

French et al. (2004) (hereafter referred to as FMD04) analyze runoff from a 100-year, 24-hour precipitation event into RDL with the objective of comparing the runoff for both normal and hydrophobic soil conditions. FMD04 conclude that that hydrophobic conditions do not increase runoff.

FMD04 use California Data Exchange Center's meteorological data and linear regression to relate elevation to annual average temperature and precipitation. Similar approach is used to contrive a point-based 100-year, 24-hour storm from National Oceanic and Atmospheric Administration (NOAA)'s 100-year, 24-hour precipitation depths of gauging sites in the watershed draining into RDL. As for the subbasin properties, soil type and vegetation density is analyzed to partition the watershed into five-elevation based sub-basins in accordance with elevation definitions defined by the US Forest Service.

In order to calculate the runoff from precipitation and subbasin characteristics, FMD04 apply the runoff curve number, an analytical approach developed the Natural Resource Conservation Service (NRCS), formerly the Soil Conservation Service (SCS). This approach depends on the calculation of curve

number that is dependent on the land-cover and soil type. Its use in hydrologic modeling is prevalent throughout the world. Nayak and Jaiswal (2003) use it to estimate storm runoff in the Besbas river basin in India. Melesse and Shih (2002) use GIS, remote sensing, and the NRCS curve number method to estimate runoff depth on the Kissimmee River basin in Florida.

This study expands on the French et al. (2004, 2006) studies by using satellite data for land-cover and percent impervious surface area and USGS's surveyed soil data to calculate the curve number. Furthermore, the model itself is considerably more detailed as there are 98 subbasins with unique precipitation values and basin properties, including the curve number, for each subbasin. The study uses historical data to calibrate channel loss. Furthermore, the model also includes anthropogenic structures such as flood control structures which retain flood flows. Due to the added complexity of the model, hydrologic software developed by the U.S. Army Corps of Engineers Hydrological Engineering Center (HEC-HMS) is used to carry out the simulations.

Chapter 3: Data and Methods

The primary objective of this research is to develop a rainfall-runoff model to predict water volume in RDL. Such determination depends on the consideration of relevant processes as well as spatial and temporal conditions. Successful modeling requires an accurate representation of the physical watershed characteristics, precipitation observations, and runoff processes.

3.1 Process Overview

The advent of GIS and the recent availability of remotely sensed, satellite-based data have contributed to significant advances in hydrologic modeling. There are two different models developed in this study: a traditional model resembling FMD04 and a computational model. The watershed in both the models is delineated using a GIS application. Runoff calculations in the traditional model are performed by hand but in the computational model, Hydrologic Engineering Center's Hydraulic Modeling System (HEC-HMS) is used to estimate runoff volume. This section contains a brief description of the models and the building process while a detailed description is available in Appendix A.

Delineating the watershed in GIS involves the use of a Digital Elevation Model (DEM), stream network for the area of interest and a project point (inlet to RDL in this study) (Figure 4). DEMs are three dimensional representation of the Earth's terrain. Such data are either derived from USGS's National Elevation Dataset constructed from topographic Quad maps or from remotely sensed satellite data. Stream network data is built from USGS's Quad maps that are corrected and updated based on satellite imagery.

The process of watershed delineation in GIS is driven by flow direction, as flow takes the path of the steepest gradient, and a user specified outlet (inlet to RDL in this study). A detailed description of watershed delineation procedure is provided in Appendix B. The delineated watershed has 98 sub-basins connected by 63 flow channels.
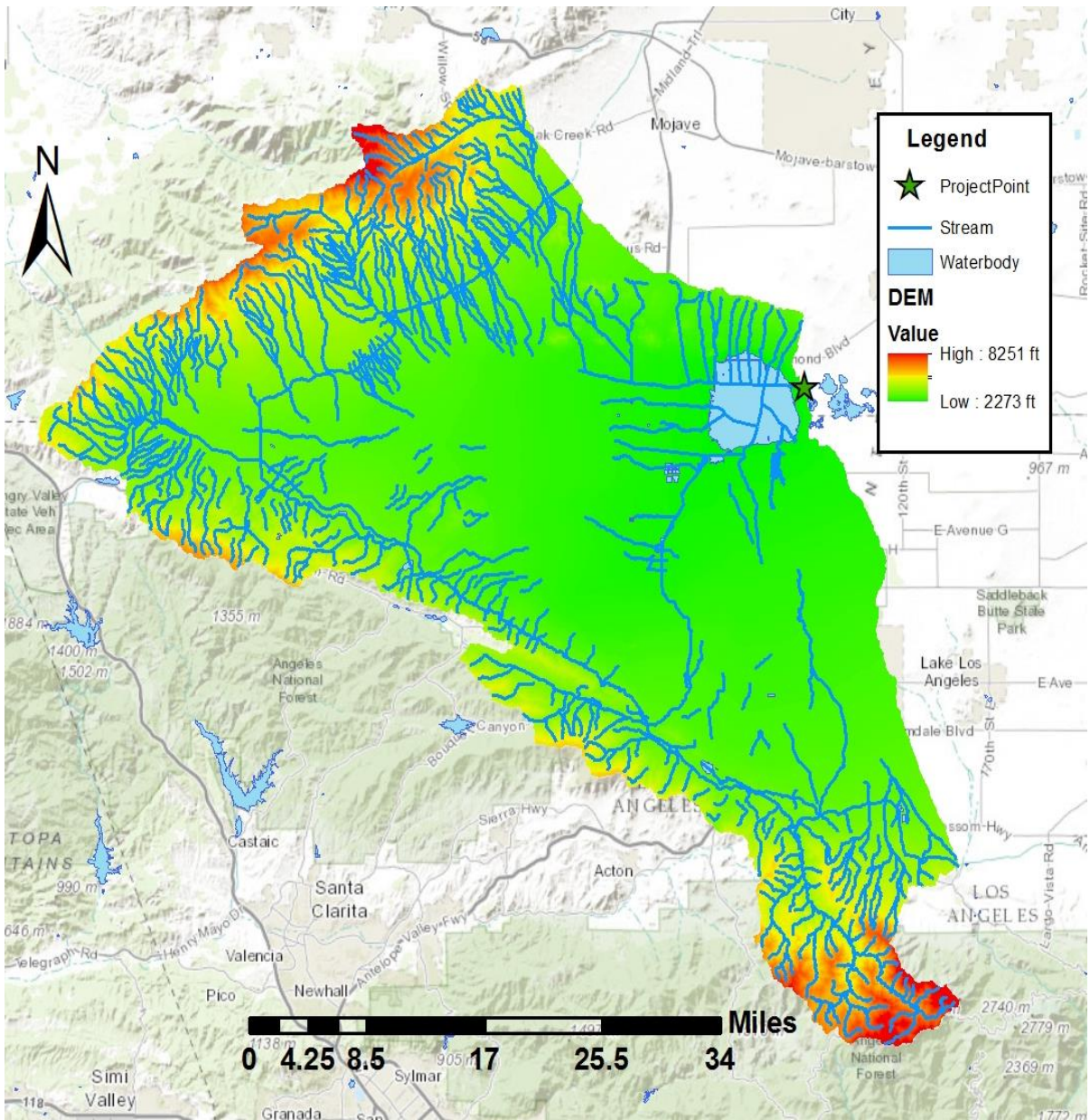
Figure 4: The DEM (the elevation grid), Stream Network (blue lines), user defined watershed outlet (green star) and the water bodies present in the watershed as visible in ArcMap.

In order to calculate the curve number, each sub-basin is assigned a hydrologic soil group, land cover type and percent impervious surface area (Figure 5). Soil information is retrieved from soil maps available in the Soil Survey Geographic (SSURGO) dataset; land cover and percent impervious surface area information is derived from National Land Cover Database 2006 (NLCD 2006) based on the Landsat Enhanced Thematic Mapper+ (ETM+) circa 2006 satellite data and has a spatial resolution of approximately 100 ft (Fry et al., 2006).
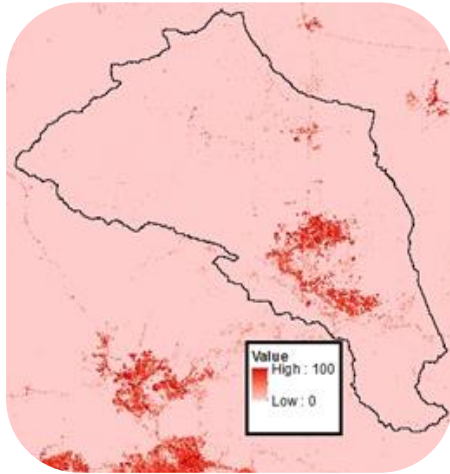
Percent Impervious Surface
Area
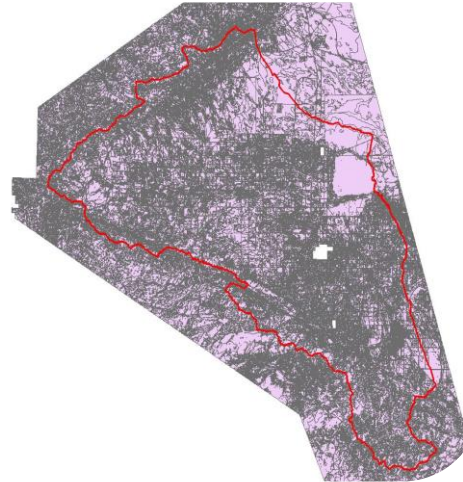
Land Cover and Soil Type
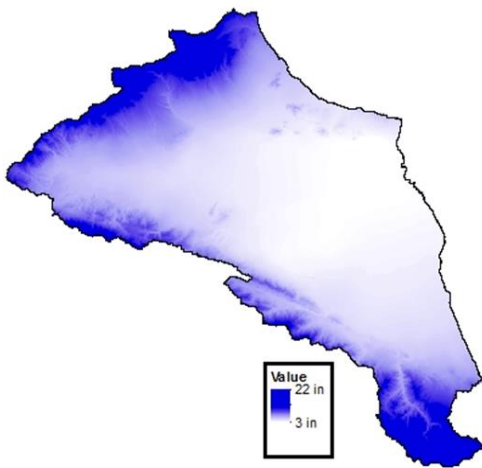
100-Year, 24-Hour
Precipitation
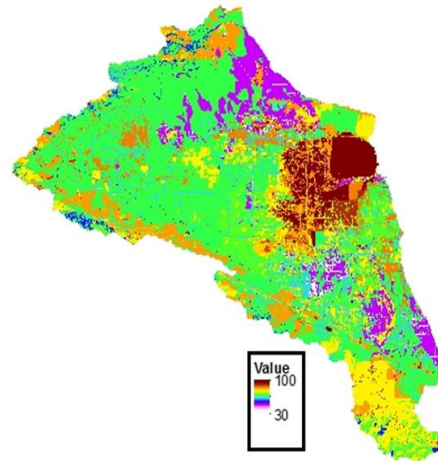
Curve Number
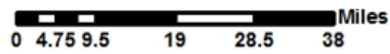
Figure 5: Images of maps and grids used in the development of the model.

Before exporting the model to HEC-HMS, spatially varying precipitation of approximately 0.6 mi spatial resolution from the Daymet dataset is assigned to each subbasin. Daymet implements a collection of software and algorithms to iteratively interpolate and extrapolate from spatially referenced precipitation observations of meteorological data to produce gridded estimates (Thornton et al., 2012).

3.2 Runoff Modeling and the NRCS Curve Number Method

Rainfall-runoff models are hydrological tools that simulate runoff resulting from a storm event. They are used to provide an understanding of a watershed's response to climatic variables, plan flood protection and manage water resources (Beven, 2012). A plethora of such models have been in use since the early 1960s (Todini, 1988). Beven (2012) classifies runoff models into two categories: lumped and distributed. Lumped models treat catchment (watershed) as a single unit with state variables represented as averages while distributed models consider the catchment as a series of sub-catchments or grid-cells such that spatial heterogeneities can be represented and are generally more process-based (Beven, 2012). Semi-distributed models share characteristics with both these types of models. The runoff curve number method applied in this study is an example of a semi-distributed model.

The NRCS-CN method is an analytical approach to calculate storm runoff. It was developed by the NRCS in 1954 to study runoff in small watersheds for the prevention of soil erosion after the passage of the Flood Control Act of 1936 (Singh, 1982). Curve number is the empirical relationship (curve) between annual runoff and precipitation (Huggins and Monke, 1968). Developed in the 1950s, it is still widely used in hydrologic modeling due to the availability of relevant data, usability and its acceptance in the United States and abroad (Garen and Moore, 2005). While the method is designed for a single continuous precipitation event, discontinuous events can be simulated through the modification of CN based on antecedent soil moisture (Woodward et al., 2002).

The NRCS-CN approach uses land-cover, soil type, hydrologic condition, and antecedent soil moisture to estimate direct runoff (channel runoff, surface and subsurface flow) based on non-point precipitation. The curve number can range from 0 to 100, 0 implying maximum infiltration and no runoff while 100 implies zero infiltration and maximum runoff. For instance, heavily urbanized cities with minimal pervious surfaces are likely to have a curve number closer to 100.

The NRCS-CN approach differentiates rainfall from effective rainfall. When it rains over a watershed, not all of the rainfall contributes to the runoff. Some of the water enters the soils through

infiltration and some of it is lost to initial abstractions (intercepted by plants and puddled in depressions). Effective rainfall is actual rainfall minus initial abstractions and infiltration.

Cumulative runoff (*Q*) is computed according to the following relationship:

$$Q = \frac{(P - I_a)^2}{(P - I_a + S)}$$ [1]

where *Q* = accumulated runoff depth over drainage area*, P* = accumulated rainfall depth over the drainage area, I_a = Initial abstractions (e.g., depression storage, interception), and *S* = Potential maximum detention of water by soil (mostly infiltration). *S* is based on CN according to:

$$S = \frac{1000}{CN} - 10$$ [2]

where *CN* = Curve number

$$I_a = 0.2 \times S$$ [3]

From the above relationships, the following conclusions regarding the NRCS-CN method can be made:

- *P* and runoff *Q* are directly proportional, i.e., more rainfall means more runoff;
- I_a and *S* are inversely proportional to *Q*, i.e., higher values I_a or *S* result in lower values of *Q*;
- I_a and *S* are inversely related to CN, i.e., higher CN implies lower values of I_a and *S*, and consequently,
- I_a and *S* are dependent on the land cover and soil type. These values are typically high for good hydraulic conductors such as sand. On the other hand, clay, which has a very slow rate of water transmission, has low values for both I_a and *S.*

There are different ways of calculating the CN. If the *P* and subsequent *Q* are known, then the CN can be calculated from Figure 2-1 or Table 2-1 in TR-55. Otherwise, knowledge of the land cover and soil type is adequate in determining CN from Table 2-2 in TR-55.

The NRCS-CN approach was chosen for this study for several reasons. Firstly, it is widely accepted in the field of hydrology. It is also a standard in commonly used runoff models such as HEC-HMS. Secondly, it provides the right level and can be refined later in the future. For instance, calculation

of sub-basin parameters like basin lag time and initial abstractions require field experiments but they can also be estimated from the curve number. Lastly, data (soil and landuse) necessary for the calculation of CN are readily available.

While NRCS-CN method is widely used and accepted, it contains several deficiencies. The most notable being that it is independent of time, i.e. it only accounts for the total runoff volume and not intensity and duration (Mockus, 1972). Similarly, spatial variability is traditionally not considered. However, in modern approaches, including this study, spatial variability can be represented by dividing the watershed into smaller sub basins each with their own values for precipitation and land characteristics. Lastly, because the method was developed mainly for agricultural land cover, it performs best in such landscapes and not as well when applied to other land cover types (Hawkins, 2009).

Despite these deficiencies, various studies have validated the accuracy of the NRCS-CN method in predicting direct runoff. For example, Melesse and Graham (2004), after comparing runoff volume calculated using the NRCS-CN method with observed data, determine that the method is able to predict the threshold precipitation required to induce runoff with 98% accuracy. Liu and Li (2008) use the NRCS-CN method to calculate the runoff volume in the Wangdonggou watershed during the period of 1996 and 1997 and estimate runoff to 75% accuracy. A similar study applied to RDL performed by French et al. (2006) corroborates these findings without quantifying the accuracy.

In the case of this study, availability of high resolution satellite data makes the implementation of CN approach feasible at the sub-basin scale. The curve numbers and precipitation mapped for each sub-basin provide HEC-HMS the necessary data required to perform the simulations.

3.3 Historical Runoff Volume Based on Satellite Imagery

A model's performance is measured by its ability to reproduce observed data. Water volume data are usually available in the form of gauge readings. However, there are no suitable data available for RDL. Hence, a new approach is developed to estimate water volume based on Landsat images and LIDAR data of RDL. Landsat images are photographs of the lake taken from satellites while LIDAR is a technology which uses sensors to measure distances. The spatial resolution of the LIDAR generated DEM of the lake is approximately 3 ft.

In order to calculate runoff volume in the lake, two Landsat images are required: one before the storm and one after. The inundated area from the image before the storm is subtracted from the

inundated area of the image after the storm to determine the increase in inundated area caused by the storm (Figure 6). This area is then used to determine a corresponding volume based on an area-volume relationship graph for RDL (Figure 7) developed by Simone Evett, an undergraduate student at Loyola Marymount University. Landsat satellites take pictures of a location once every 16 days. But since precipitation events in the region last no more than a handful of days, a daily evapotranspiration rate of 0.04 in, based on CIMIS (2000), is applied to the cumulative precipitation. Due to the lack of a relationship between evaporation and inundated area, the effects of evaporation on the water in the lake is overlooked. It has to be noted that for the pool of historical events considered in this study, the difference between the end of a storm and the second Landsat image is no more than 4 days. Other losses such as infiltration are considered negligible. In addition, this study does not consider flow from the LWRP to RDL, which typically occurs from mid-fall to mid-spring for the simulated scenarios. Compared to rainfall-runoff, the flow from LWRP is negligible.

Water Volume After the Storm (13 Dec 1992) − **Water Volume Before the Storm (27 Nov 1992)** = **Water Volume Caused by the Storm**
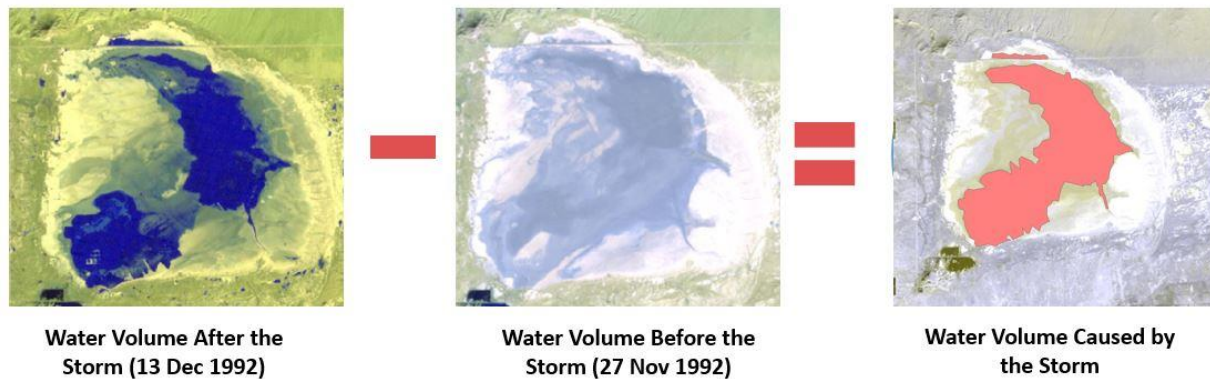
Figure 6: Process for calculating the runoff caused by a storm event using satellite images of RDL before and after a storm event.
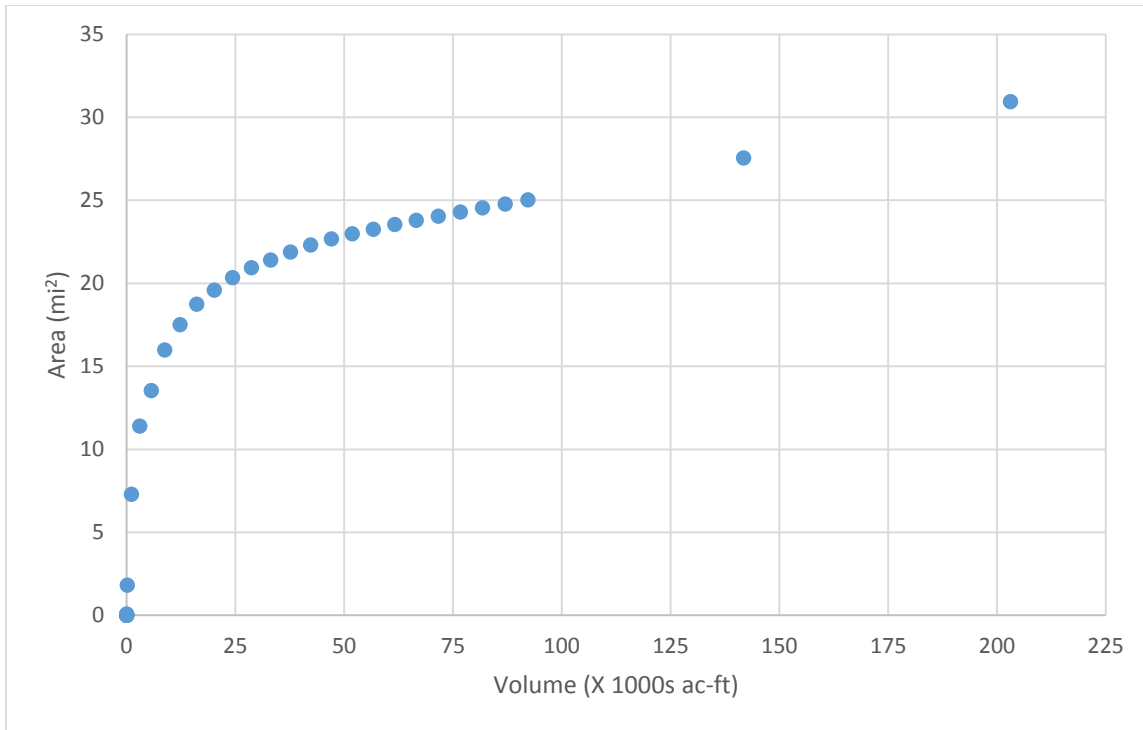
Figure 7: Wet Area-Volume relationship for RDL developed by Simone Evett, Loyola Marymount University.

Landsat satellites started taking images of the Earth's surface since 1982, but only ten historical events are selected. There are various reasons behind this. First, only images encompassing a precipitation event completely could be used as it takes time for runoff from various parts of the watershed to reach the lake. Secondly, more often than not, clouds would hover over RDL, this inhibited the use of the image. Thirdly, if the Daymet precipitation data corresponding to an event is missing, the image could not be used. And lastly, if the image is taken more than four days after the precipitation event, the event is not considered. This is done to minimize the effects of evaporation and infiltration on the water in the lake.

3.4 Hydrologic Model – HEC-HMS

Given a series of corresponding variables, HEC-HMS is capable of simulating the rainfall-runoff process for a dendritic watershed with a known stream network. It also possesses the ability to separate and mathematically model different processes of the surface water cycle using a variety of parameters. In this study, the NRCS-CN method is used to estimate runoff losses in the watershed. Transmission losses are modeled using a constant fractional loss method based on the climatic index (CI), a function of temperature and precipitation, and sub-basin area (Mockus, 1972). This approach of calculating

transmission loss requires the calculation of sub-basin specific basin lag time (time difference between peak of rainfall and peak of runoff), which is computed based on the curve number:

$$T_l = max \left(\frac{L_s^{0.8} \ [(1000/CN)-9]^{0.7}}{31.67 \ S^{0.5}}, 3.5 \times \Delta t \right) \qquad [4]$$

where T_l is the sub-basin lag time in hours, L_s is the length of the sub-basin's longest flow path in feet, *CN* is the sub-basin's curve number, *S* is the slope of the sub-basin's longest flow path and Δt is the time step of the simulation in hours.

The HEC-HMS configuration developed for the RDL watershed is a network of 98 sub-basins and 63 flow channels (Figure 8). Each channel reach contains unique values for length, slope and fractional transmission loss coefficient. All reaches have identical routing parameters. Each subbasin contains unique values for slope, basin lag time, precipitation, percentage of impervious surface area and curve number (based on soil type and land cover). The precipitation can be changed to reflect different storm events. The raw data corresponding to these parameters are manipulated to make them compatible with HEC-HMS. A detailed parameter list is provided in Appendix C. The simulation features a 15 minute time step and lasts for a duration of 72 hours with all precipitation occurring in the first 24 hours. The extra time allows runoff from various parts of the watershed to reach the lake. In addition, there are three iterations of this model, dry, normal and wet, with different sets of curve numbers corresponding to different antecedent moisture condition.
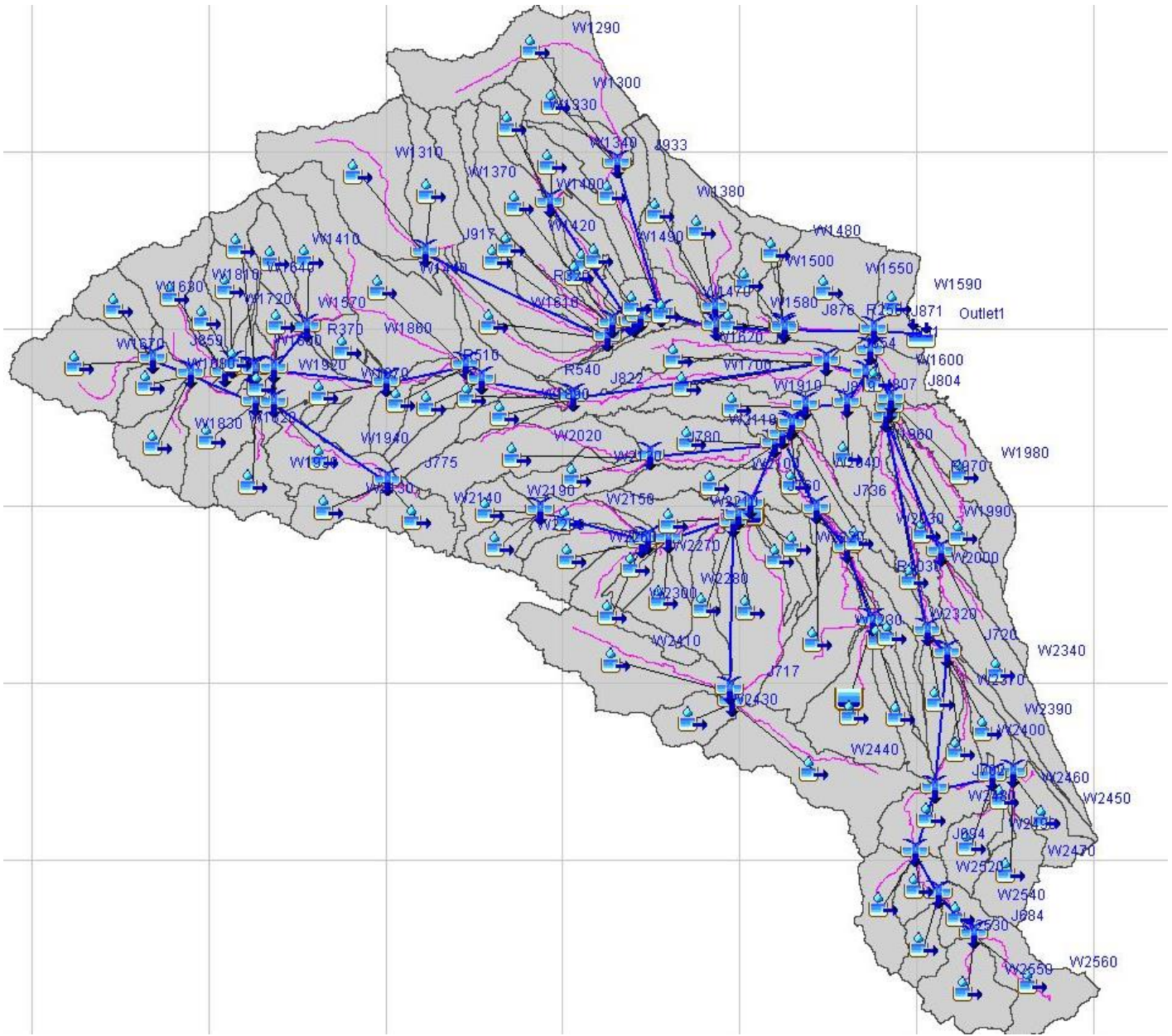
Figure 8: The watershed model as viewed in HEC-HMS. The blue lines represent the network of channels while the black lines, the sub-basin boundaries. The pink lines represent the rivers.

Precipitation

Spatially varying precipitation is required to model storm-runoff using the CN method. There are two different precipitation grids used in this study: historical and derived (elevation-based). The historical storm is derived from the Daymet dataset. The precipitation is converted to a continuous storm event based on the unit hyetograph for the region available in Los Angeles County Hydrologic Model (LACHM) (Figure 9) (Conkle et al., 2006). Both Daymet and the 100-year precipitation is available as daily values, but since HEC-HMS accepts continuous precipitation only, this change is necessary. Modifying the precipitation in this way affects the shape of the hydrograph (timing of the runoff) at RDL but it does not affect the total runoff volume. The derived storm is constructed using the following relationship developed by FMD04:

$$P_{100} = 3.55 + 0.0031\,(E - 2302) \tag{5}$$

where P_{100} is the 24-hour 100-year precipitation in inches and E is Elevation in feet. P_{100} is 3.55 inches at RDL (2302 ft is the official elevation. It is different than the 2275 ft mentioned earlier. Our observation of LIDAR data of RDL puts the lake at 2273 ft above sea level) and increases with elevation. As with the daily precipitation grid, the temporal distribution of the hyetograph is determined according to the LACHM (Conkle et al., 2006) (Figure 9). The shape of the hyetograph, however, does not affect the final runoff volume.
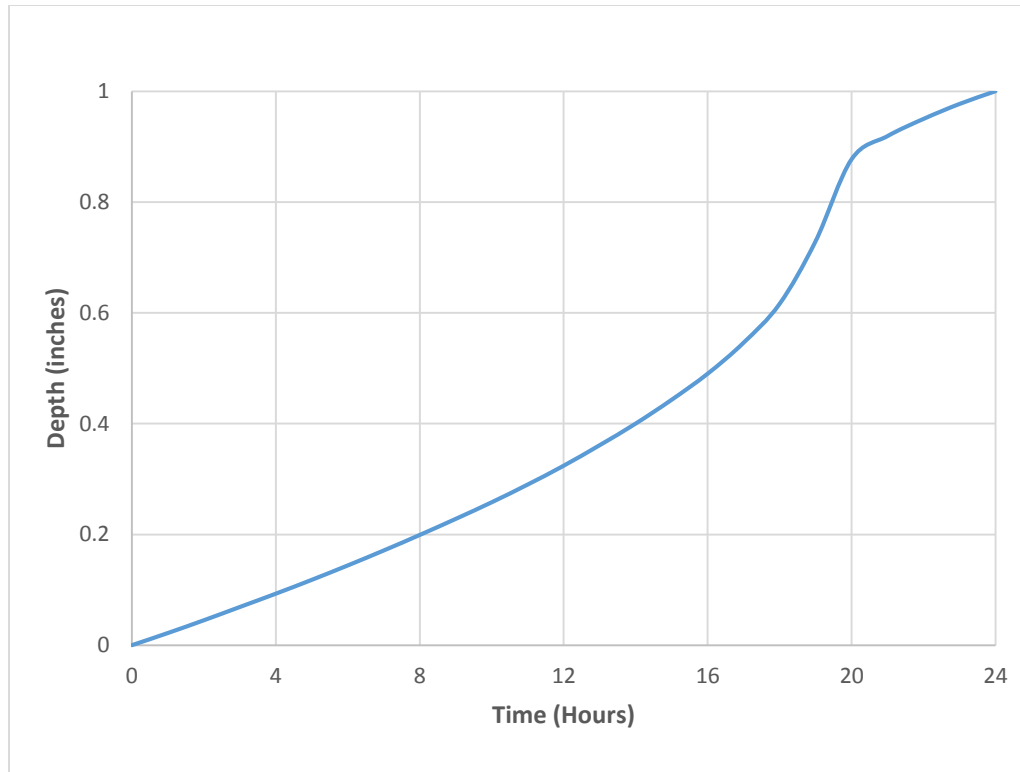
Figure 9: 24-hour unit hyetograph for the study area as recommended in LACHM (Conkle et al., 2006).

Antecedent Moisture Condition (AMC)

The degree of wetness of soil is directly proportional to runoff volume. AMC is a measure of this wetness. Furthermore, the curve number of a soil is dependent on its AMC. A soil is able to retain more water when it is dry (low AMC) than when it is damp (high AMC). Hence, a soil has a low curve number when it is dry, a higher curve number when is damp and highest when it is wet. The NRCS-CN method accounts for this phenomena by providing three different values, adjusted for dry, wet and normal conditions, for the curve number at any given spatial coordinate.

In this study, the AMC is determined by referring to Table 2 available in the National Engineering Handbook (NRCS, 1971). This table categorizes AMC based on antecedent precipitation index (API), i.e., accumulated precipitation over a preceding five day period (Mockus, 1972 as cited in Mishra, 2003). This helps decide the set of curve numbers (dry, normal or wet) to be assigned to the watershed. A value less than 0.5 in means dry AMC condition, while a value more than 1.1 in means wet. For this model, cumulative precipitation on the preceding day is compared with this relationship to find the AMC of a given day. Satellite images of the watershed before the start of the storm are also analyzed before assigning the AMC.

In order to account for evaporation from the soil, 0.04 in is subtracted from the cumulative precipitation for days when there is no rain. A detailed table of the categorization of AMC for ten historical storms is provided in Appendix C, and an example is presented in Table 3.

Table 2: Antecedent Moisture Condition (AMC) classification based on total accumulated precipitation according to the National Engineering Handbook, Section 4 (1972).

AMC	Total five-day antecedent rainfall (in)
I (Dry)	Less than 0.5
II (Normal)	0.5 to 1.1
III (Wet)	More than 1.1

Table 3: Categorization of AMC based on cumulative precipitation values (0.04 in is subtracted for days with no rain) of the previous day.

Date	Precipitation (in)	Evaporation (in)	Cumulative Precipitation (in)	AMC
26-Nov-97	0.46	0.00	0.46	Dry
27-Nov-97	0.23	0.00	0.69	Dry
28-Nov-97	0.00	0.04	0.65	Norm
29-Nov-97	0.00	0.04	0.61	Norm
30-Nov-97	0.22	0.00	0.83	Norm
1-Dec-97	0.26	0.00	1.08	Norm
2-Dec-97	0.00	0.04	1.04	Norm
3-Dec-97	0.00	0.04	1.00	Norm
4-Dec-97	0.00	0.04	0.96	Norm
5-Dec-97	0.39	0.00	1.35	Norm
6-Dec-97	2.55	0.00	3.90	Wet
7-Dec-97	0.11	0.00	4.01	Wet
8-Dec-97	0.12	0.00	4.13	Wet

Evapotranspiration (ET)

Over land, evaporation and transpiration are the two phenomena that constitute evapotranspiration. In a hydrological context, evaporation is the loss of water from soils and water surfaces while transpiration is the loss of water stored in plants (Heldman, 2003). The California Irrigation Management Information System (CIMIS), has developed a location-specific reference evapotranspiration table for California based on historical average estimations from a Class A

evaporation pan and the Penman-Monteith relationship (University of California Cooperative Extension and California Department of Water Resource (UCCE & CDWR), 2000). Since evaporation affects runoff volume via a reduction in soil moisture, a value of 0.04 inches of daily evaporation is assigned to the entire watershed based on the average reference evapotranspiration values for the watershed developed by CIMIS (UCCE & CDWR, 2000).The evapotranspiration is subtracted from the cumulative precipitation to determine the AMC of the watershed for a given day.

Transmission Loss

Water lost as runoff travels downstream in a channel constitutes transmission loss. This includes seepage into groundwater, ponding in flood plains and evaporation (National Engineering Handbook, Chapter 18, 2007). In some instances, however, groundwater contributes to the stream and there is a gain. Since the watershed considered in this study is arid, gains are ignored. Transmission losses are related to time and runoff (Kabbes, 2007). The accuracy of runoff model is dependent on transmission losses, but the spatial variation of antecedent moisture condition, precipitation, and evaporation rates affect transmission loss. The most accurate means of incorporating channel losses is through gaged readings of different channels during a storm. Hence, theoretical estimates of channel losses are, in most cases, calibrated based on known values of rainfall and consequent runoff.

An approach developed by NRCS, that requires the computation of the climatic index (*CI*) and area for each sub-basin to estimate fractional transmission loss coefficient (FTLC) for direct runoff, is applied (Mockus, 1972). The method implements an empirical coefficient, FTLC, which calculates the abstractions using a fixed loss ratio. The ratio can range from 0 to 1, with 1 implying no loss and 0 implying 100% loss. The table to estimate the reduction factor is available in the Appendix C while the formula to calculate climatic index is as follows (Mockus, 1972):

$$CI = \frac{100 \times P}{T^2}$$
[6]

where *P*= average annual precipitation in inches and *T*= average annual temperature in Fahrenheit.

The runoff volume calculated using this set of values significantly underestimates, by over 200%, what the Landsat images predict. Hence, these values are adjusted using an iterative process to align runoff calculations with Landsat estimates. These iterations are carried out on a subset of four storms whose precipitation ranges from 1.6 in to 4.6 in. All events except the February 1996 (4 days) are 8 days

long. After analyzing the runoff volumes for various fractions of FTLC (Table 4 and Figure 10), 61% of the actual FCLC is concluded to be the best estimate in the case of this watershed.

Table 4: Runoff comparison for ChanLoss_FM. Of the three sets of values for FTLC, 61% is used in the FM.

Date	Runoff (ac-ft)			
	Landsat	88% of FTLC	61% of FTLC (FM)	50% of FTLC
Dec-91	3,400	12,500 (270)	3,200 (-6)	2,000 (-40)
Feb-96	3,000	9,300 (210)	2,700 (-10)	1,500 (-50)
Jan-08	4,100	22,600 (450)	5,900 (44)	3,900 (-5)
Feb-09	1,800	1,700 (-6)	900 (-50)	600 (-70)
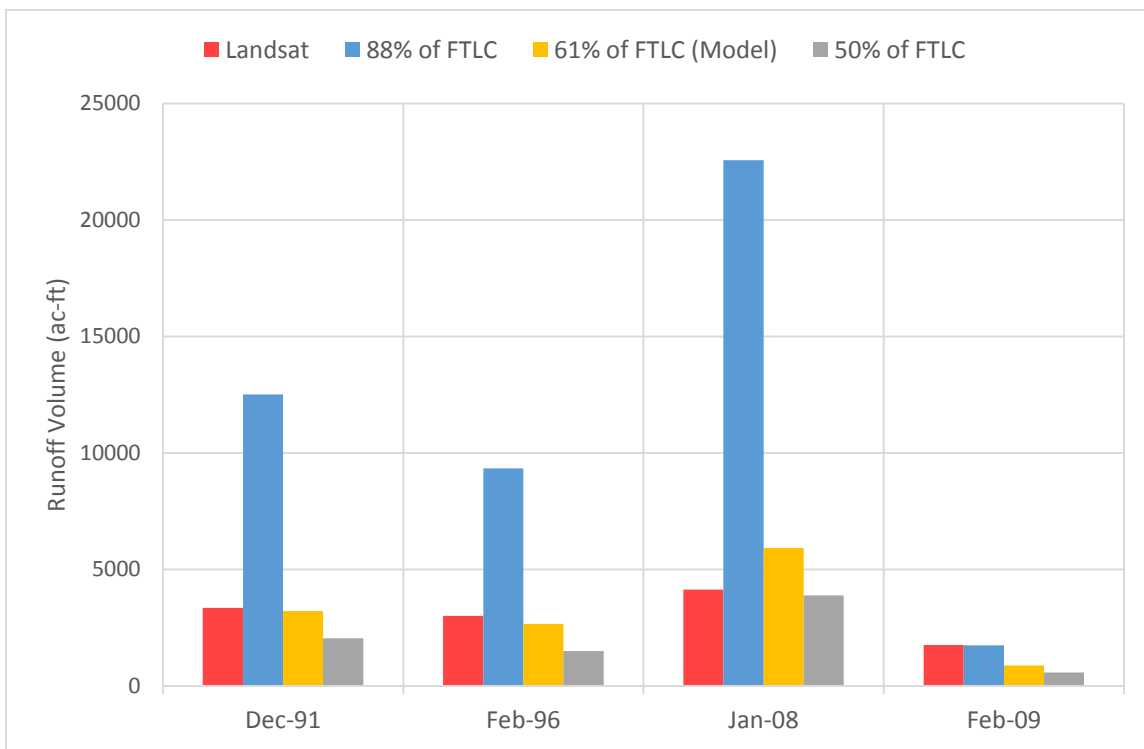
Figure 10: Runoff comparison for various fractions of FTLC.

Flow Routing

Flow routing is the process of determining the runoff hydrograph at any given point in the watershed (Mays, 2011). It helps determine the impact of channel characteristics on runoff. Due to the fact that the calculation of transmission losses in HEC-HMS depends on routing, it is imperative to assign a reach routing method to the FM despite the lack of channel data. There are various methods for routing flow in a watershed. In this study, the flow is routed using the Muskingum method.

The Muskingum method was developed in the 1930s while designing fold control schemes for the Muskingum River Basin in Ohio (McCarthy, 1938). It is based on the principle of conservation of mass and depends on two coefficients (Equation 7): travel time (*K*), the storage coefficient which can be estimated as the time it takes for flow to travel through the channel reach, and weighing factor (*x*), a dimensionless storage factor that determines the influence of inflow, for instance a value of 0 for *x* indicates minimal inflow influence (most likely a reservoir).

$$S = K[XI + (1 - X) \, O] \hspace{3cm} [7]$$

where *S* = Storage in ft³, *K* = travel time in hours, *x* =storage factor, and *I* = Inflow ft³/s. *O* = Outflow in ft³/s:

Since transmission losses are a constant fraction of the flow in the method used in this study, the Muskingum routing parameters have no effect on the final runoff volume. They do, however, modify the shape of the hydrograph, which is not considered in this study. For example, if the losses are 10% for a given channel and occur in one time-step, for a total flow of 100 ac-ft, the loss is 10 ac-ft (10% of 100 ac-ft). However if runoff comes in two time-steps in 30 ac-ft and 70 ac-ft, the loss is still 10 ac-ft (10% of 30 ac-ft + 10% of 70 ac-ft).

Detention Basins

Detention basins are surface structures designed to detain water for a specific amount of time in order to attenuate the flow of storm water (Sustainable Stormwater Management, 2009). They help avoid floods and consequent soil erosion (Sustainable Stormwater Management, 2009). The city of Lancaster contains 37 detention basins with a combined storage capacity of 7,100 ac-ft. The city of Palmdale also has numerous detention basins but their storage capacity was unavailable at the time of the research. For simplicity, the numerous detention basins are lumped into one structure for each city. As a result, two detention basins, one with a capacity of 7,100 ac-ft for Lancaster and another with a capacity of 5,000 ac-ft for Palmdale are included in the model.

3.5 Design of Experiments

Two versions of the model are created for this study. One to validate the delineation process and grid-derived hydrological parameters, the other to study the effects of urbanization on storm

runoff. A variety of simulations are carried out in these two models (Table 5). The simulations are described in the upcoming sections.

Table 5: List of simulations carried out in this study. Precipitation implies the type of precipitation data used for the simulation, while flood control implies the presence or absence of detention basins in the city of Lancaster and Palmdale. Simulations performed on the simplified model end with the suffix "SM" while all simulations performed on the full model end with "FM".

Simulation Name	Model	Precipitation	Detention Basin
NoSR_SM_P100	Simplified	100-Year, 24-Hour	No
SR_SM_P100	Simplified	100-Year, 24-Hour	No
Hist_FM	Full	Daymet Historical	Yes
NoDet_FM_P100	Full	100-Year, 24-Hour	No
NoUrbn_FM_P100	Full	100-Year, 24-Hour	No
Urbn_FM_P100	Full	100-Year, 24-Hour	Yes
Sprl_FM_P100	Full	100-Year, 24-Hour	Yes

Simplified Model

The first version of the model created is the simplified model (SM). It is similar to the model created in FMD04. The main purpose of this model is to verify the watershed delineation process by creating a model identical to FMD04 and comparing the runoff values. FMD04 created their model using a DEM to delineate the watershed in GIS. It was then partition the watershed into six subbasins connected by five reaches after analyzing the predominant vegetation and soil type found in the elevation intervals. Each subbasin is assigned a curve number based on soil and vegetation data. Precipitation for each sub-basin is calculated using the elevation-precipitation relationship (Equation 5) described in Section 3.4 Hydrologic Model – HEC-HMS but for average elevation of the elevation category. Finally, runoff caused by the event is calculated analytically using the NRCS-CN approach.

The SM is a network of four sub-basins and three flow reaches. It is derived from the watershed delineated in ArcMap. Although the GIS-delineated watershed has 98 sub-basins and 63 reaches, SM only has 4 sub-basins and 3 reaches. The 98 sub-basins are categorized into elevation ranges based on their centroid elevations (elevation at the center of mass or area). This is done to keep SM consistent with the model developed in FMD04. Moreover, a curve number grid from SSURGO's surveyed soil data and NLCD's satellite-based land-cover and percent impervious surface area data are added to the model. The precipitation is derived from a 33 ft grid developed using the relationship developed in FMD04 (Equation 5). Hence, curve numbers and precipitation values assigned to the sub-basins are area-based,

weighted averages from the corresponding grids created in ArcMap. The following simulations carried out in the SM are computed analytically using Microsoft Excel:

- NoSoilRet_SM (Simplified model with no soil retention storage): This simulation is carried out to validate the watershed delineation process. The runoff calculated in this study is compared with that from FMD04. The volume of water detained by the soil (S) is unaccounted for to keep consistency with Table 10 (runoff calculation in Microsoft Excel using the NRCS-CN approach) in FMD04. This is achieved by setting *S* to zero in the calculation of accumulated runoff depth over drainage area, *Q*, in equation 1.

- SoilRet_SM (Simplified model with soil retention storage): This simulation is also carried out to compare and verify the runoff and soil retention in the model and FMD04. The conditions and calculations for this simulation is the same as NoDet_PM, except the fact that *S* is considered in the calculation of accumulated runoff depth over drainage area, Q, for both Soil_Ret_SM and FMD04.

Full Model

The full model (FM) is more sophisticated than SM and is composed of a network of 98 sub-basins and 63 flow channels. It is developed to analyze the impacts of urbanization and roles of detention basins in managing storm. Similar to the SM, it also includes unique, spatially-varying curve number and precipitation values for each sub-basin. Moreover, parameters for fractional channel loss, unique to each of the 63 flow channels, and percent impervious surface area, unique to each sub-basin, are also included. Antecedent Moisture Condition (AMC) unique to each storm event and evapotranspiration for the entire watershed are also considered (See Section 3.4). To better represent current conditions, anthropologic flood control structures, specifically two "bulk" detention basins are added to represent the numerous detention basins in Palmdale and Lancaster. All FM simulations are carried out in HEC-HMS. The following is the list of simulations:

- Hist_FM (FM with historical storms): To check the model's performance, ten historical, multi-day, storms are considered using precipitation data from Daymet as input. The runoffs estimated by the model are compared with the estimates from the Landsat images.

- NoDet_FM_P100 (FM with detention basins removed): In order to analyze the effects of detention basins on storm runoff volume, both detention basins in Palmdale and Lancaster are removed and runoff is calculated for the 24-hour, 100-year, storm (Equation 5).

- NoUrbn_FM_P100 (FM with the cities removed): The cities of Palmdale and Lancaster, are removed by altering the curve (See Appendix C) to analyze storm runoff in pre-urbanized conditions. All sub-basins within the vicinity of the two cities, whose percent impervious surface area is 10% or more are assigned values of 2% and the composite curve number is calculated. The 24-hour, 100-year, storm is used.

- Urbn_FM_P100 (FM with increased urbanization): This simulation is carried out to analyze the effects of urbanization on runoff volume. The General Plan 2030 for the city of Lancaster recommends that the city be developed from within. To do so, urbanization (impervious area) is increased by 25%, 50% and 100% of the current value and the corresponding curve number is computed (composite CN) (See Appendix C).The range of curve numbers for FM is 59 to 85; with a 25% increase, the range is 60 to 86; with a 50% increase, the range is 62 to 88 and, with a 100% increase, the range is 663 to 91.The 24-hour, 100-year, storm is used.

- Sprl_FM_P100 (FM with two new cities): In this simulation, two additional sub-basins, adjacent to Lancaster and Palmdale, are urbanized to resemble urban sprawl. The percentage of impervious surface area for the new sub-basins is manipulated to be consistent with adjacent sub-basins in Lancaster and Palmdale and the corresponding curve numbers are calculated. The 24-hour, 100-year, storm is used.

Chapter 4: Data and Results

The watershed in both models are developed from the same DEM and stream network. The degree of sophistication, however, is varying. Similarly, the nature of simulations and analysis performed in the two models is also different and so are the findings. This chapter details the datasets used as inputs, modifications and assumptions made to simulate certain conditions, the resulting consequences and an analysis of the findings.

4.1 Simulations on the Simplified Model (SM)

SM, a network of four sub-basins and three channels, is developed primarily for the purpose of validating the watershed delineation process. Runoff generated by the 24-hour, 100-year precipitation event for simulations NoSR_SM_P100 and SR_SM_P100 is compared to the results from FMD04 (Figure 11).
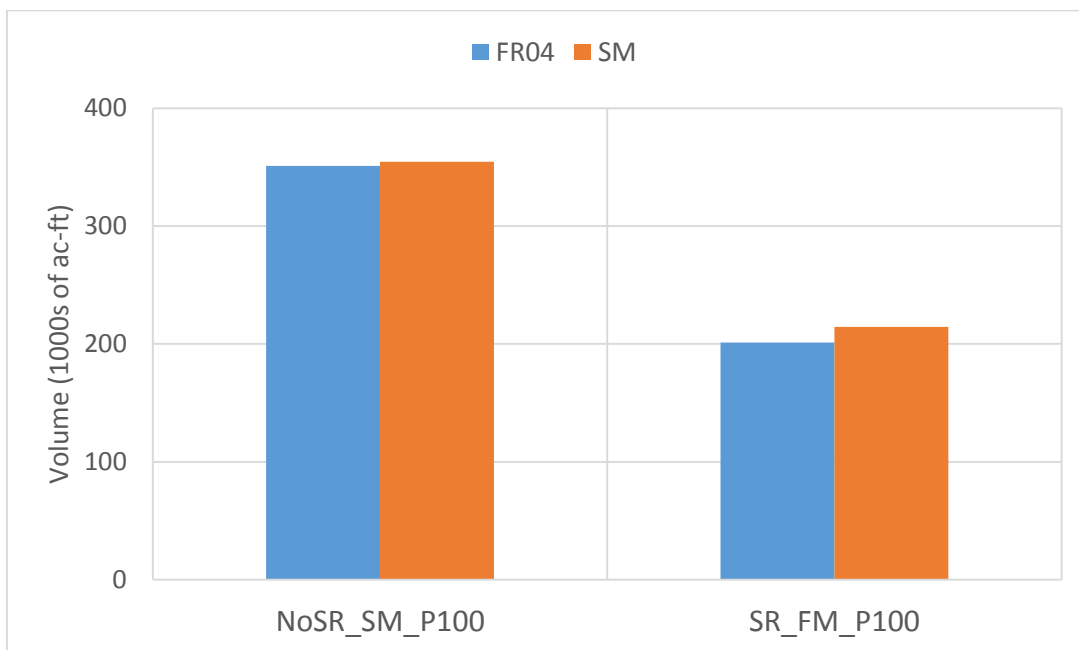
Figure 11: Runoff Comparison between FMD04 and SM.

When no soil detention is considered (NoSR_SM_P100), the SM simulates 1% more (549 ac-ft and 554 ac-ft) runoff than FMD04 (Table 6). When considering soil detention (SR_SM_P100), SM simulates 6% more (314 ac-ft and 335 ac-ft) runoff. These minor discrepancies are primarily a result of differences in the land cover and soil data sources. Consequently, the average CN for the entire watershed in FM is 73 and FMD04 is 70. Therefore, FM's higher CN results in higher runoff. FMD04's CNs

are estimated based on predominant land-cover, soil type and vegetation, while SM's are estimated from satellite-based land cover data and surveyed soils data, thus accounting for spatial variability.

Table 6: Comparison of key hydrological parameters in FR04 and SM. Since the sub-basins are categorized based on elevation ranges, average values for lowest and highest elevation are mentioned.

Parameters	FR04	SM
Watershed Area (sq. mi)	1200	1200
Lowest Average Elevation (ft)	2500	2600
Highest Average Elevation (ft)	7600	5300
Average CN	69	72
Average Precipitation (in)	6.4	6.3
Runoff (NoSR_FM) (ac-ft)	549	554
Runoff (SR_FM) (ac-ft)	314	335

The similarity in the runoff volume between these simulations, NoSR_SM_P100 and SR_SM_P100, and FMD04 validates the GIS-based watershed delineation carried out in this study as well as the datasets and the implementation of the NRCS-CN approach.

4.2 Simulations on the Full Model (FM)

Once the delineation process is verified, the model is further refined. Parameters representing percentage of impervious surface area, flood control structures, evapotranspiration, antecedent moisture condition (AMC), flow routing and transmission loss (Table 7) are added to create a refined version of the SM, the Full Model (FM). Since the simulations on the FM are carried out in HEC-HMS, the initially delineated watershed is left intact.

An essential component to the model is the representation of AMCs, transmission loss and channel routing.

Table 7: Range of Hydrological Parameters in the Full Model.

Parameter	Minimum	Maximum
Curve Number (Dry)	37	80
Curve Number (Normal)	56	89
Curve Number (Wet)	74	94
Channel Loss Coefficient	0.68	0.79
Evapotranspiration (in/day)	0.04	n/a
Percent Impervious Surface	0.01	34
Palmdale Detention Basin (acre-foot)	n/a	7000
Lancaster Detention Basin (acre-foot)	n/a	5000

4.2.1 Model Verification

Historical storms of varying duration and intensity are used to calibrate the model. Four events, Dec-91, Feb96, Jan-08 and Feb-09, are used for the calibration of transmission loss while the rest were simulated independent of calibration.

The shortest storm, February 2004, lasts for 3 days while the longest storm, January 1998, lasts for 10 days. Incidentally, these two storms are also the lower and upper extremes. The February 2004 storm measures 0.9 in and the January 1998 storm measures 5.6 in. The results, in general, are as expected with smaller precipitation events inducing smaller runoff volumes and vice versa (Table 8). There are, however, two notable discrepancies. First, the 1998 storm that occurred during the strongest El Niño on recent record and is the largest storm in the dataset. It, however, renders 7400 ac-ft of runoff – a smaller than expected value. A possible source of this discrepancy could be snow. Precipitation data from Daymet includes both snowfall and rainfall, but only rainfall induces instant runoff while snow melts over the course of time. Hence, the disproportionate runoff. The second major discrepancy is the 1992 storm of 2.9 inches, which induces less runoff than the 2.6 inch storm of 1996. The lapse times for the 1992 and 1996 events are one and two days, respectively. It is possible that some of the runoff from the 1992 event is yet to reach Rosamond Lake. Moreover, historical meteorological data shows that the temperature during the 1996 event was higher than the temperature during the 1992 event which implies varying evaporation rates.

Table 8: Runoff volume estimation based on Landsat images. Columns 1 and 2 are the dates when the images were taken. Column 3 is the average wind speed on the day when the post-storm image was taken and 4 is the wind temperature in RDL during the period between the pre-storm image and post-storm image. Column 5 is the cumulative precipitation during that time while column 6 is the lag between the end of the storm and the final Landsat image date, 2. And finally, column 7 is the runoff caused by the event.

1	2	3	4	5	6	7
Pre-Storm Date	Post-Storm Date	Post-Storm Average Wind Speed (knots)	Average Temperature in RDL (°F)	Cumulative Precipitation (in)	Lapse (days)	Landsat Runoff Volume (ac-ft)
27-Dec-91	12-Jan-92	1	42	4.0	4	3,400
27-Nov-92	13-Dec-92	9	44	2.9	1	2,100
8-Feb-96	24-Feb-96	12	55	2.6	2	3,000
25-Nov-97	11-Dec-97	10	44	4.1	3	8,400
28-Jan-98	13-Feb-98	5	46	5.6	4	7,400
21-Jan-04	6-Feb-04	4	44	0.9	2	1,200
14-Dec-04	30-Dec-04	10	44	4.2	0	11,300
16-Jan-08	1-Feb-08	15	41	4.6	3	4,100
3-Feb-09	11-Feb-09	10	45	1.6	3	1,500

7-Dec-10	23-Dec-10	5	50	5.3	0	13,300

Biases between the runoff from Landsat and the FM ranged between +/- 12% except for two events (Figure 12). The model overestimated runoff for November 1997 and January 2008 by 59% and 44%, respectively.

Various factors contribute to the large bias observed for the two events including snow, wind, and evaporation. In addition, changes in the shape of the water body also introduces error in the Landsat-based volume. During the 2008 event, the average wind speed on the post-storm image date is 15 knots at an average azimuth of 240°. The presence of sand dunes on the northeast part of the lake are indicative of the fact that strong wind push the water in the northeast direction. Similarly, the average wind on the post-storm image date of 1997 event is 10 knots with an average angle of 250°. Strong winds also increase the evaporation rate as they reduce the humidity close to the water surface and also disrupt the molecular bonds in water. November 1997 also marked the start of the El Niño. Furthermore, there are days when the temperature at various parts of the watershed is below 32°F (freezing point), such low temperatures are indicative of snow. Since both rainfall and snowfall are lumped as a single parameter in Daymet, and only rainfall causes runoff the model is bound to overestimate. The precipitation dataset contains values interpolated based on readings made by precipitation gauges. However, there is temporal and spatial variation in precipitation. Moreover, factors like rainfall intensity are not incorporate in the model.
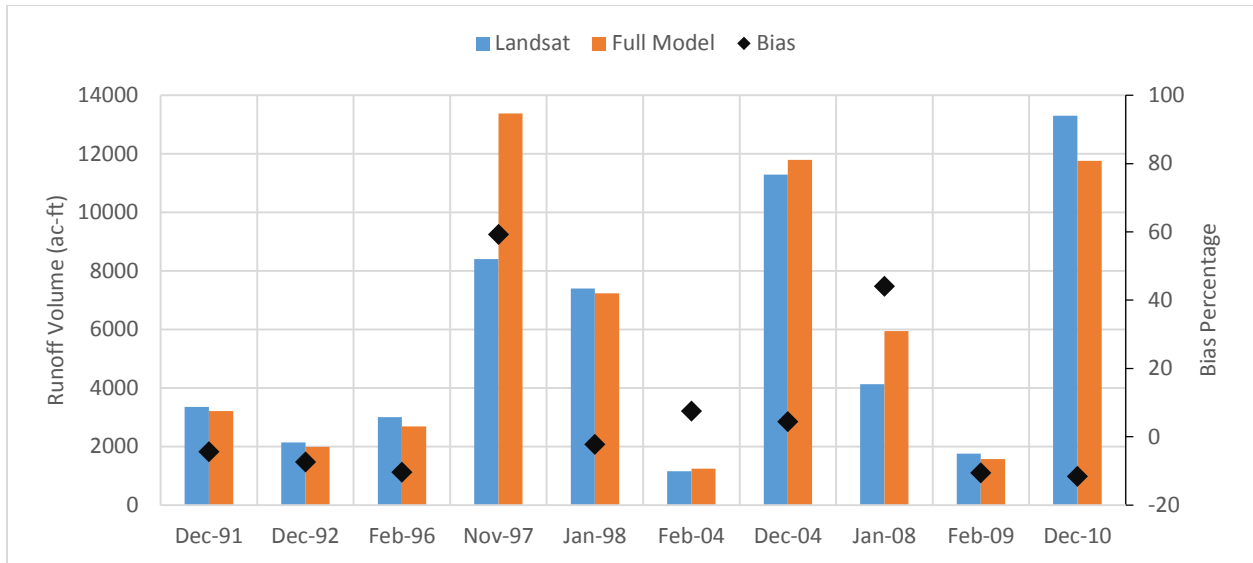
Figure 12: Runoff comparison between the full model and the Landsat estimates. The left axis denotes runoff volume while the right denotes the percentage difference between the two volumes.

In summary, the model performed considerably well with the exception of two events. It is an effective tool that can be used for a variety of applications.

4.2.2 The Role of Detention Storage

Lancaster and Palmdale have numerous storm detention basins distributed throughout the cities. In FM, these structures are lumped into two detention basins with approximate capacities of 7,000 ac-ft for Lancaster and 5,000 ac-ft for Palmdale. To analyze the effect of flood control structures on storm runoff, both detention basins in Palmdale and Lancaster are removed, while other parameters are left unaltered (NoDet_FM_P100).

For present conditions, the 100-year, 24-hour precipitation induces a runoff of 3,300 ac-ft. Even though the two detention basins collectively store 3,700 ac-ft, removing them increases the runoff into RDL by 300 ac-ft only (Table 9, Figure 13). This is because most of the 3,700 ac-ft is lost during transmission. In the model, the detention basins are located outside the cities (downstream), hence, no change is noticed in the runoff generated by the subbasin representing the cities. And due to the placement of the detention basins, not all subbasins representing the city drain into them. As a result of this, even though the detention basins have a combined storage capacity of 12,000 ac-ft, throughout the course of this research, there is only one instance when a detention basin overflows.

Table 9: Runoff comparison between the FM in present conditions and FM with the detention basins removed (NoDet_FM).

Subbasin	Area (mi²)	Present Conditions		NoDet_FM_P100
		Runoff (ac-ft)	Storage (ac-ft)	Runoff (ac-ft)
W2030	14	1,300		1,300
W2100	13	1,500		1,500
W2110	17	1,700		1,700
W2160	6	600		600
W2210	13	1,100		1,100
W2220	5	600		600
W2230	22	1,900		1,900
W2240	9	1,100		1,100
W2250	25	2,600		2,600
W2270	5	500		500
W2280	8	900		900
W2300	10	1,600		1,600
W2310	5	400		400
W2320	8	500		500
W2350	6	500		500
W2360	19	2,500		2,500
W2370	9	500		500
W2430	8	2,200		2,200
Outlet (RDL)	**n/a**	**33,000**		**33,300**
Lancaster Detention Basin	n/a	0	1,200	n/a
Palmdale Detention Basin	n/a	0	2,500	n/a

4.2.3 Impacts of Urbanization on Storm Runoff

This is achieved by altering CN, percent impervious surface area and the status of flood control structures (detention basins) in the basins are altered to analyze the watershed's response to urbanization. Since flood control structures are generally designed to accommodate large events, only the effects of 24-hour, 100-year storm in runoff is considered.

The urbanized areas in the cities of Palmdale and Lancaster sub-basins are removed from the FM (NoUrbn_FM_P100) by lowering the percent impervious surface area and modifying the corresponding curve number for the sub-basins that lie within the vicinities of Lancaster and Palmdale. Subbasins whose percent impervious surface area exceed 10% are lowered to 2%. A threshold of 10% is selected as composite curve numbers stop fluctuating below that point. A value of 2% is chosen after

analyzing the percent impervious surface area of undeveloped areas in the watershed. Seven out of eighteen sub-basins are modified (Table 10). The two detention basins are also removed from the model as they did not exist before the development of the cities.

Table 10: Table of variables and runoff for FM and NoUrbn_FM_P100. Note that the manipulated sub-basins are highlighted in blue.

Sub-basin	Full Model (FM)			NoUrbn_FM_P100		
	CN	% Impervious	Runoff (ac-ft)	CN	% Impervious	Runoff (ac-ft)
W2030	77	2	1,300	77	2	1,300
W2100	85	3	1,500	85	3	1,500
W2110	81	0.5	1,700	81	0.5	1,700
W2160	68	34	600	60	2	200
W2210	76	4	1,200	76	4	1,200
W2220	69	30	600	60	2	200
W2230	64	12	1,900	60	2	1,200
W2240	72	22	1,100	60	2	500
W2250	68	21	2,600	60	2	1,300
W2270	75	0.2	500	75	0.2	500
W2280	71	18	1,000	60	2	500
W2300	73	0.9	1,600	73	0.9	1,600
W2310	68	4	400	68	4	400
W2320	66	6	500	66	6	500
W2350	61	9	500	61	9	500
W2360	70	21	2,500	60	2	1,200
W2370	59	1	500	59	1	500
W2430	75	1	2,200	75	1	2,200

Removing the cities decreased total runoff (Figure 13). Although the collective runoff from the sub-basins representing Palmdale and Lancaster fell from 10,300 to 5,100 ac-ft, the final runoff decreased by 80 ac-ft only.

Most of the 5,200 ac-ft of runoff is lost during transmission. Secondly, detention basins curtail the effects of urbanization on runoff. From the previous simulation (NoDet_FM_P100), it is concluded that the detention basins reduce the runoff by 300 ac-ft. This is corroborated by the fact that the difference between the runoff generated by the version of the model without detention basins (NoDet_FM_P100) and the version without cities (NoUrbn_FM_P100) is 360 ac-ft.
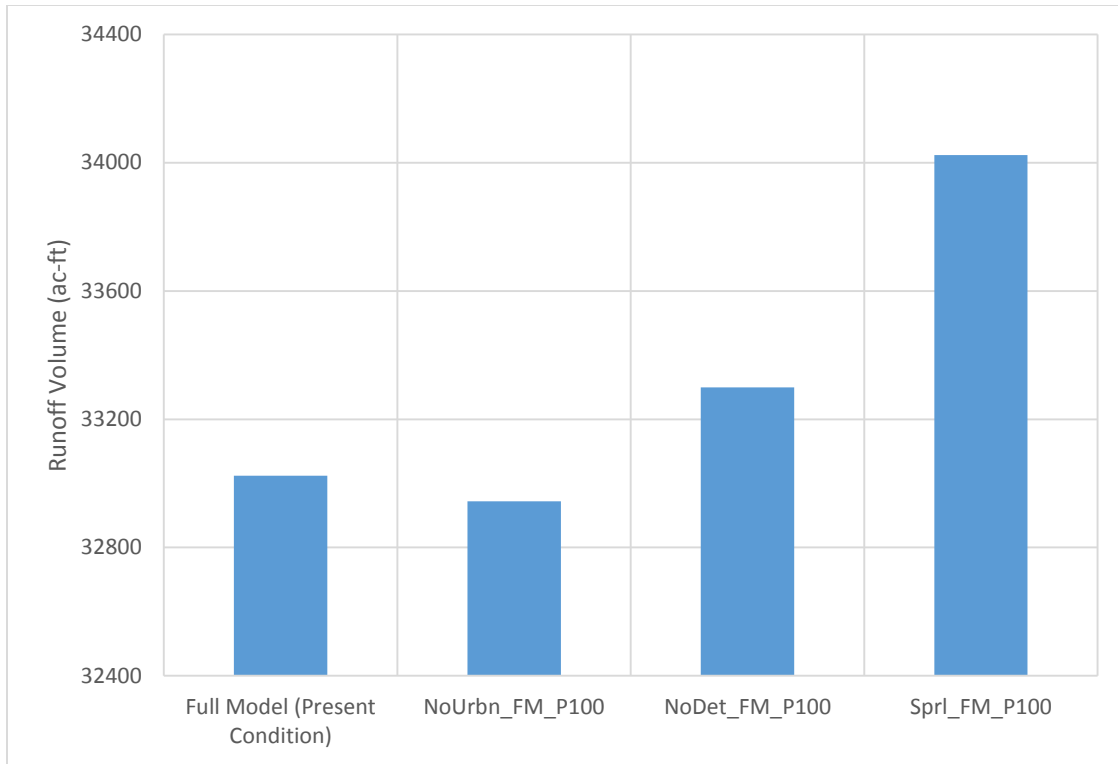
Figure 13: Total runoff comparison between the Final Model, NoUrbn_FM_P100, NoDet_FM_P100 and Sprl_FM_P100.

4.2.4 Impacts of Urbanization Trends in Lancaster and Palmdale

Urban sprawl is a trend of low-density land development on and beyond the edges of central cities (Squires, 2002). An alternatives to sprawl is infill (high-density development that involves undeveloped areas inside a city and building vertically), which is also the suggested development strategy in the Lancaster General Plan 2030. The impacts of these two different strategies on storm runoff volume are analyzed using FM.

In order to simulate sprawl (Sprl_FM_P100), areas on the outskirts of the cities of Lancaster and Palmdale are urbanized by altering the percentage of impervious surface area and the corresponding curve number (Table 11). The percent impervious surface area is increased to 24 as the average percent impervious surface area of the seven most developed subbasins representing the cities (W2160, W2220, W2240, W2250, W2280, and W2360) is 24.The curve number is graphically determined from the composite curve number method provided in TR-55. The parameters of the subbasins representing the cities of Lancaster and Palmdale are left unaltered to isolate the impacts of the newly developed areas. Lastly, no modifications are made to the two detention basins in the FM and no new flood control structures are added in Sprl_FM_P100.

38

Table 11: Table of variables and runoff for FM and Sprl_FM_P100. Note that only the manipulated sub-basins are included.

Sub-basin	Full Model (FM)			Sprl_FM_P100		
	CN	% Impervious	Runoff (ac-ft)	CN	% Impervious	Runoff (ac-ft)
W1960	86	0.6	1,700	88	24	2,100
W2110	81	0.5	1,700	84	24	2,300
W2120	69	0.2	700	77	24	1,300
W2150	71	0.1	700	78	24	1,100
W2200	75	0.1	1,000	80	24	1,400
W2340	65	0.4	1,500	73	24	2,800
W2390	66	3.0	700	74	24	1,100
W2400	67	4.0	700	75	24	1,000
W2410	74	1.0	7,300	79	24	9,000
W2440	73	3.0	6,100	79	24	7,800
W2480	75	0.5	3,000	80	24	3,800
Outlet (RDL)			33,000			34,000

The results from Sprl_FM_P100 indicate that sprawl increases runoff. Although, the cumulative, runoff for the manipulated sub-basins increases by 8,600 ac-ft (from 25,100 ac-ft to 33,700 ac-ft), the final runoff into RDL increases by 1000 ac-ft only. Once again, the reduction from 8,600 acre-ft at the sub-basin level to 1,000 acre-ft in RDL can be attributed to transmission losses. It should also be noted, that the newly-urbanized sub-basins in Sprl_FM_P100 constitute 13% of the entire watershed.

The General Plan 2030 for the city of Lancaster recommends developing undeveloped areas within the city instead of areas outside the city. Due to the lack of information regarding Palmdale's development, it is assumed that the city adapts a similar approach. In order to simulate this scenario, the undeveloped areas within the vicinity of Lancaster and Palmdale are urbanized (Urbn_FM_P100) by increasing the percentage of impervious surface area by 25%, 50% and 100%.

The increase in runoff associated with the increase in urbanization is proportional to the increase in impervious surface area. Areas with higher impervious area induce higher runoff and vice versa (Table 12). Increasing the percentage of impervious surface area in the cities of Lancaster and Palmdale by 25%, 50% and 100% increases the sub-basin specific runoff and total runoff by 3,300 acre-ft and 180 acre-ft, 6,600 acre-ft and 390 ac-ft and 1,000 acre-ft and 640 ac-ft respectively.

Table 12: Sub-basin specific runoff comparison for various degrees of internal urbanization.

Sub-basin	Full Model		25% Increase in Impervious Area			50% Increase in Impervious Area			100% Increase in Impervious Area		
	CN	Runoff (ac-ft)	CN	Runoff (ac-ft)	Runoff Ratio	CN	Runoff (ac-ft)	Runoff Ratio	CN	Runoff (ac-ft)	Runoff Ratio
W2030	77	1,300	78	1,300	0.00	79	1,400	0.08	80	1,500	0.15
W2100	85	1,500	86	1,600	0.07	88	1,700	0.13	91	1,900	0.27
W2110	81	1,700	81	1,700	0.00	81	1,800	0.06	82	1,800	0.06
W2160	68	600	80	8,00	0.33	88	1,000	0.67	95	1,100	0.83
W2210	76	1,200	77	1,200	0.00	79	1,300	0.08	81	1,400	0.17
W2220	69	600	80	700	0.17	88	900	0.50	94	1,000	0.67
W2230	64	1,900	70	2,400	0.26	77	3,000	0.58	83	3,600	0.89
W2240	72	1,100	78	1,300	0.18	86	1,600	0.45	91	1,800	0.64
W2250	68	2,600	75	3,300	0.27	84	4,200	0.62	90	4,900	0.88
W2270	75	500	76	500	0.00	76	500	0.00	76	500	0.00
W2280	71	1,000	77	1,200	0.20	83	1,400	0.40	87	1,500	0.50
W2300	73	1,600	74	1,600	0.00	74	1,600	0.00	75	1,700	0.06
W2310	68	400	70	400	0.00	72	400	0.00	73	500	0.25
W2320	66	500	69	600	0.20	72	700	0.40	74	800	0.60
W2350	61	500	65	600	0.20	69	700	0.40	75	900	0.80
W2360	70	2,500	78	3,200	0.28	84	3,700	0.48	90	4,200	0.68
W2370	59	500	60	600	0.20	62	600	0.20	63	700	0.40
W2430	75	2,200	76	2200	0.00	76	2,200	0.00	78	2,300	0.05
Outlet		33,000		33,200	0.01		33,400	0.01		33,700	0.02

With increased urbanization, the volume of water stored in the flood control structures (detention basin) increases due to less infiltration (Figure 14). Increasing the percentage of impervious surface area in the cities of Lancaster and Palmdale by 25% increases the volume of water stored in the detention basins by 1,000 ac-ft, a 50% increase increases the detention storage by 1,900 ac-ft while doubling percentage of impervious surface area (100% increase) increases storage by 2,400 ac-ft. For the 25% and 50% increase cases, the detention basin did not overflow. For the 100% increase, however, the detention basin in Palmdale overflowed. These results confirm that detention basins are effective in compensating for increases in storm runoff caused by change in land use due to urbanization.
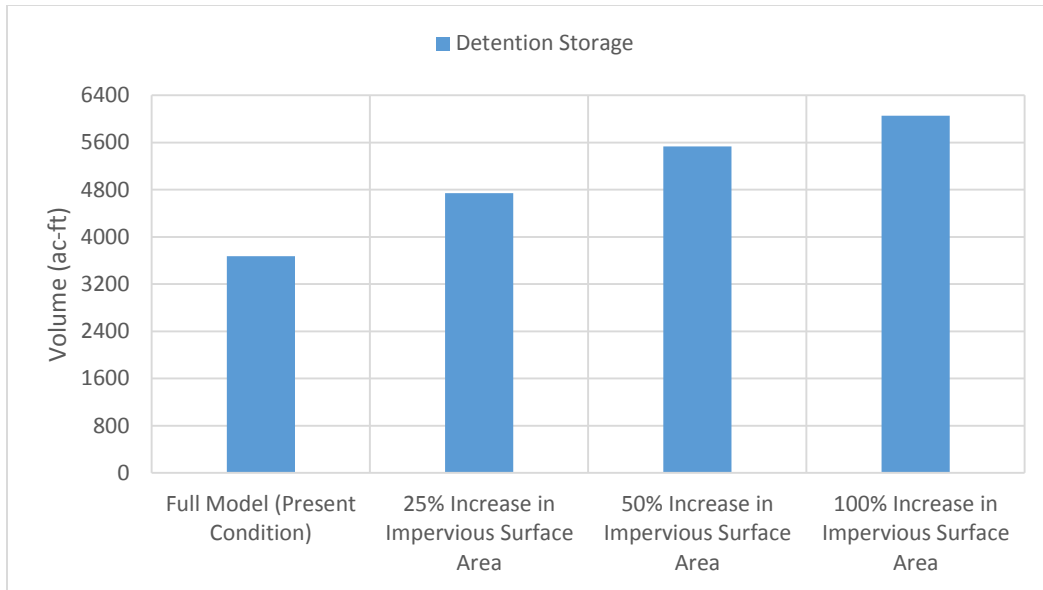
Figure 14: Detention storage comparison for various levels and trends in urbanization. The bars represents the volume of water stored in the detention basins of the cities of Lancaster and Palmdale.

The runoff from infill (internal urbanization) is compared to the runoff from sprawl (outward urbanization) to study the impacts of these two different urbanization trends on storm runoff (Figure 15). Even doubling the infill urbanization induced less runoff than urban sprawl. It should be noted, however, that in the case of sprawl (Sprl_FM_P100), no additional flood control structures are added to the newly developed areas.
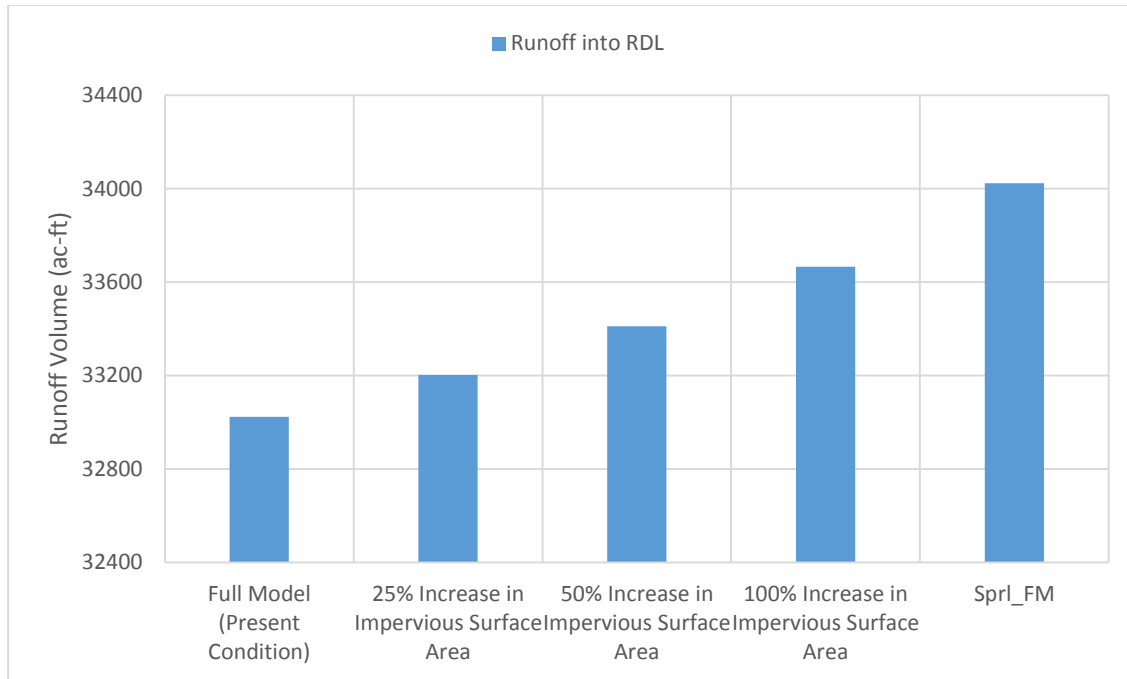
Figure 15: Runoff comparison for various levels and trends of urbanization. The blue bars represent runoff volume and the black dots represents the change compared to the full model.

Chapter 5: Conclusions, Future Recommendations and Caveats

In this study several state-of-the-science datasets are utilized to construct two rainfall-runoff models, Simplified Model (SM) and Full Model (FM), which estimate the storm runoff into RDL. SM is developed to validate the watershed delineation process and also to compare the results with a similar study performed on the lake, FMD04. SM contains four sub-basins and three channels. FM is a more refined version of the SM. It is a network of 98 sub-basins, 63 flow channels and two detention basins and includes unique values representing spatially-varying curve numbers, precipitation and percent impervious surface area for each sub-basin and transmission loss and routing in each channel. Furthermore, antecedent moisture condition (AMC) unique to each precipitation event's pre-storm conditions for the entire watershed is also considered. The FM is developed to study the effects of urbanization and the role of flood control structures, specifically detention basins, on storm runoff based on a 100-year, 24-hour storm event developed in FMD04. Simulations on the FM are performed in HEC-HMS.

Despite using different datasets, the results from the SM and FMD04 are similar. In fact, for two different simulations, the SM overestimates by 1% and 6% only. Any discrepancy between the two

42

studies stems from the difference in datasets and approach. The similarity of the results validate the delineation process implemented in this model.

Due to a lack of gaged data for the volume of water in RDL, Landsat images are analyzed to estimate runoff. These estimates are later used to calibrate transmission loss parameters in FM. A comparison of the simulated runoff to the Landsat estimates demonstrates a bias range of +/- 12% for eight of the ten simulated historical storm events. There are two events whose estimates are considerably higher: 59% in November 1997 and 44% in January 2008. It is likely to have been caused by the effects of snow and wind. Daymet's data indicates that, during the 2008 event, snow fell on certain parts of the watershed. This however is not the case for the 1997 event. However, for both cases, wind affects the shape of the water body and influences the evaporation rate, both these factors affect the water volume calculation in RDL. The time gap between the end of a storm and the Landsat image amplifies the effect of evaporation and wind effect on the final runoff. Despite these deficiencies, the model performs remarkably well in simulating storm runoff into RDL.

Several simulations are performed on the two aforementioned models. The findings from the study affirm the hypotheses of the study:

- The curve number approach coupled with satellite data is effective in estimating runoff.
- Past urbanization in desert regions has increased runoff.
- In cities, infill generates less additional runoff than sprawl in cities.

In addition to the hypotheses, the following conclusions can also be drawn from the findings:

- Satellite-based data provides a promising and innovative method to estimate storm runoff volume in RDL and other playas and terminal lakes. Moreover, satellite images provide an effective means for estimating water volume in lakes and playas.
- Transmission losses reduce storm runoff. One of the main factors influencing transmission loss in the method used in this study is average annual temperature. Hence, an increase in annual temperature increases channel losses and consequently reduces storm-runoff.
- Both urbanization approaches (infill and urban sprawl) increase runoff. On the subbasin level, runoff almost doubles. However, most of it is lost during transmission.

43

The following caveats should be considered regarding the models developed in this study:

- Due to the lack of gauged data, satellite images are used to estimate runoff accumulated in the lake. These images are taken once every sixteen days. Consequently, a gap, sometimes, exists between the last day of a storm and the day the pictures are taken. This lapse ranges from zero to four days. Moreover, the volume calculated from this process is an estimate as adequate gauge data were not available for comparison.
- Both models do not consider inflow from LWRP and infiltration in RDL. These flows are believed to be negligible in comparison to the runoff generated by the storms.
- There is a time difference between the start and end of a precipitation event and the two corresponding satellite images. It is assumed that the water lost due to evaporation before and after a storm is commensurable. Hence, water lost from the lake due to evaporation is unaccounted for. A water balance model of the lake is currently being constructed to address this issue.
- Wind influences the rate of evaporation and is also known to change the shape of a water-body. These effects of wind are also overlooked.
- Despite the high spatial resolution of the DAYMET precipitation data, it is interpolated from a sparse network of precipitation gages in the watershed. This can potentially result in substantial errors in model input.
- Daymet's precipitation is measured in in/day. These values are then fitted on a hyetograph provided in the LA Country Hydrological Manual. Issues such as rainfall intensity, which can considerably affect amount of storm-runoff are overlooked.
- Snow often occurs in the mountains during the winter months. Precipitation input into the model does not separate snowfall and rainfall. This can potentially result in an overestimate in runoff since snowfall does not induce storm-runoff.
- The pre-storm snow conditions can significantly modify the characteristics of storm-runoff.
- There are deficiencies in the NRCS-CN method. Of particular note, it does not account for the intensity or duration of the storm (Mockus, 1972). Moreover, since it was developed for agricultural land-cover, it doesn't perform well when applied to other land cover types (Hawkins, 2009).

- Transmission losses are estimated using a constant fractional loss method. The effect on losses due to the temporal distribution of flow is over looked as the method implies that transmission losses are a function of volume only.

- Due to the lack of runoff gages, transmission losses are estimated using a climatic index. While this method results in favorable estimates, it also results in significant errors.

- There are thirty-seven different detention basins in the city of Lancaster. In the model, they are represented by one detention basin outside the city. Although the capacity of the model's detention basin is the same as the actual, lumping the thirty-seven basins together misrepresents the storage in and runoff from these detention basins as the large detention basins are less likely to overflow.

- The detention basins are assumed to be empty prior to a storm, which in reality may not be the case. The amount of water stored in the basins prior to a storm is influential in estimating runoff into RDL.

- In order to calculate AMC, the entire watershed is assigned a singular daily evaporation rate. This is likely to cause minor discrepancies as factors, like soil type, vegetation and land cover that affect AMC are spatially varying.

Despite the aforementioned caveats, the model performs well in predicting storm runoff into RDL. To further develop the model, the following improvements are suggested:

- Although the method of using satellite images to estimate runoff is innovative, it is untested. Actual gauged data for the runoff entering RDL would be required to verify the method, as well as better verify the model.

- A more advanced and thorough procedure should be considered to model transmission loss and calibrate channel routing coefficients. This would likely require the installation of runoff gauges throughout the basin.

- Replacing singular bulk detention basin with smaller individual basins is likely to improve the capabilities of the model.

- In the model, RDL is the only natural sink for the watershed. However, there are several other sinks and small dams within the watershed. For the purposes of this study, it is assumed they are full and do not contribute to runoff. To improve the model, these sinks should be considered.

- Developing a water balance model of RDL would assist in the analysis of evaporation and infiltration that occurs in the lake as evaporation and infiltration are occurring in the time lapse between the day the satellite images are taken and the beginning and ends of the storms.
- The NRCS-CN approach to calculate storm runoff is an event based method. A process that incorporates the temporal variability of precipitation should also be considered.

References

"About Edwards: History: The Dry Lake Beds." Edwards Dry Lake Beds. Edwards Air Force Base Public

Affairs, 25 July 2006. Web. 20 Sept. 2013.

"Arc Hydro Tools Version 2.0 User's Manual." ArcGIS Resources. N.p., 12 Oct. 2011. Web. 25 Oct. 2013.

"Background." National Elevation Dataset. USGS, Aug. 2006. Web. 25 Oct. 2013.

"CNPS Inventory Plant Detail." CNPS Inventory Plant Detail. California Native Plant Society, n.d. Web. 05

Jan. 2014.

"Description of Soil Survey Geographic (SSURGO) Database." NRCS Soils. Soil Survey Staff, Natural

Resources Conservation Service, United States Department of Agriculture, n.d. Web. 25 Oct.

2013.

"Dust Control Services - Antelope Valley Resource Conservation District." Antelope Valley Resource

Conservation Disctrict (AVRCD), n.d. Web. 22 Mar. 2014.

"Final Environmental Impact Report for Lancaster Water Reclamation Plant 2020 Facilities Plan (May

2004)." LACSD Website. Environmental Science Associates, May 2004. Web. 11 Nov. 2013.

"Historic First: Edwards AFB Lakebed Fly-In." EAA News Historic First: Edwards AFB Lakebed Fly-In.

Experimental Aircraft Association, 6 Oct. 2010. Web. 08 Jan. 2014.

<http://web.archive.org/web/*/http://www.eaa.org/news/2010/2010-10-06_Edwards-

FlyIn.asp>.

"Lancaster Water Reclamation Plant." Lancaster Water Reclamation Plant. Sanitation Districts of Los

Angeles County, n.d. Web. 1 Nov. 2013.

"Piute Ponds Edwards AFB." Piute Ponds Edwards AFB. Friends of Piute Ponds, n.d. Web. 08 Nov. 2013.

"Playa Lakes." Home. US EPA, 2012. Web. 22 Sept. 2013.

"Stormwater 101: Detention and Retention Basins." Stormwater 101: Detention and Retention Basins.

      Sustainable Stormwater Management, 28 May 2009. Web. 20 Nov. 2013.

Alderman, David, Arturo Keller, Nikki Maciejowski, Julie Randall, and Robert Shirley. "Management

      Recommendations for Piute Ponds Edwards Air Force Base, California." Master Document.

      University of California, Santa Barbara Donald Bren School of Environmental Science and

      Management, n.d. Web.

Baker, Victor R. "Playa (geology)." Encyclopedia Britannica Online. Encyclopedia Britannica, 1988. Web.

      20 Sept. 2013.

Beven, Keith J. Rainfall-Runoff Modeling: The Primer. Chichester, UK: J. Wiley, 2001. Print.

Briere, Peter R. "Playa, playa lake, sabkha: Proposed definitions for old terms." Journal of Arid

      Environments 45.1 (2000): 1-7.

Chandler, John. "Heavy March Rains Resuscitate the Dormant Desert Shrimp." Los Angeles Times. Los

      Angeles Times, 26 Apr. 1991. Web. 03 Dec. 2013.

Conkle, Chris, Janelle Moyer, Ben Willardson, Adam Walden, Iraj Nasseri, Martin Araiza, Thuong Do, and

      Peter Imaa. Hydrology Manual. Riverside, CA: Riverside County Flood Control and Water

      Conservation District, 1978. 2006 Hydrology Manual-Divided. Los Angeles Country Department

      of Public Works, Jan. 2006. Web. 14 Aug. 2013.

      <http://dpw.lacounty.gov/wrd/publication/engineering/2006_Hydrology_Manual/2006%20Hyd

      rology%20Manual-Divided.pdf>.

Cronshey, Roger, Richard H. McCuen, Norman Miller, Walter Rawls, Sam Robbins, and Don Woodward.

  Urban Hydrology for Small Watersheds (TR-55). Washington, D.C.: U.S. Dept. of Agriculture, Soil

  Conservation Service, Engineering Division, 1986. Print.

Cronshey, Roger. Urban hydrology for small watersheds. US Dept. of Agriculture, Soil Conservation

  Service, Engineering Division, 1986.

Deal, Wanda. Interview. 18 Jul. 2013.

Dunbar, Brian. "NASA Dryden Fact Sheets - The Dry Lakes." NASA. NASA, 8 May 2008. Web. 30 Sept.

  2013.

Esri. What Is ArcMap?" ArcGIS Desktop. Esri, 18 Sept. 2012. Web. 25 Oct. 2013.

French, Richard H., and Julianne J. Miller. Flood Hazard Identification and Mitigation in Semi- and Arid

  Environments. Singapore: World Scientific, 2012. Print.

French, Richard H., et al. "Use of remotely sensed data to estimate the flow of water to a playa lake."

  Journal of hydrology 325.1 (2006): 67-81.

French, Richard H., Julianne J. Miller, and Charles R. Dettling. "Estimating playa lake flooding: Edwards

  Air Force Base, California, USA." Journal of hydrology 306.1 (2005): 146-160.

French, Richard H., Julianne J. Miller, and Charles R. Dettling. "Flood Assessment for Rosamond Dry Lake,

  Edwards Air Force Base, California (2004)

Fry, J., Xian, G., Jin, S., Dewitz, J., Homer, C., Yang, L., Barnes, C., Herold, N., and Wickham, J., 2011.

  Completion of the 2006 National Land Cover Database for the Conterminous United States,

  PE&RS, Vol. 77(9):858-864.

Garen, David C., and Daniel S. Moore. "Curve Number Hydrology In Water Quality Modeling: Uses,

      Abuses, And Future Directions." Journal of the American Water Resources Association 41.2

      (2005): 377-88. Print.

Goudie, A. S. "Dust storms and their geomorphological implications." Journal of Arid Environments

      (1978).

Gupta, K. K., J. Deelstra, and K. D. Sharma. "Estimation of Water Harvesting Potential for a Semiarid Area

      Using GIS and Remote Sensing." Remote Sensing and Geographic Information Systems for

      Design and Operation of Water Resources Systems. Wallingford, Oxfordshire, UK: International

      Association of Hydrological Sciences, 1997. Print.

Gwynn, J. Wallace. History and Mineral Resource Characterization of Sevier Lake, Millard County, Utah.

      Vol. 6. No. 6. Utah Geological Survey, 2006.

Harris, Richard. "Dust Storms Threaten Snow Packs." NPR. NPR, 30 May 2006. Web. 22 Feb. 2014.

Harris, Richard. "Stirring Up Dust in the Desert." NPR. NPR, 31 May 2006. Web. 22 Jan. 2014.

Herbst, Chris, and Patti Kumazawa. "Two-year Drought Raises Risk of Predators Attacking Pets." Two-

      year Drought Raises Risk of Predators Attacking Pets. Edwards Air Force Base, 29 May 2013.

      Web. 08 Dec. 2013.

Huggins, L. F., and E. J. Monke. "A mathematical model for simulating the hydrologic response of a

      watershed." Water Resources Research 4.3 (1968): 529-539.

Hydrologic Engineering Center. August 2010. Hydrologic Modeling System HEC-HMS: User's Manual. U.S.

      Army Corps of Engineers, Davis, CA.

Hydrologic Engineering Center. May 2009. HEC-GeoHMS Geospatial Hydrologic Modeling Extension: User's Manual. U.S. Army Corps of Engineers, Davis, CA.

Liu, Xianzhao, and Jiazhu Li. "Application of SCS Model in Estimation of Runoff from Small Watershed in Loess Plateau of China." *Chinese Geographical Science* 18.3 (2008): 235-41. Web.

Mays, Larry W. Water Resources Engineering. Hoboken, NJ: John Wiley, 2011. Print.

McCarthy, G.T., 1938: 'The Unit Hydrograph and Flood Routing'. Unpublished. Presented at conference of North Atlantic Division, U.S. Corps of Engineering, New London, CT. US Engineering Office, Providence, RI. June 1938.

Melesse, Assefa M., and S.F. Shih. "Spatially Distributed Storm Runoff Depth Estimation Using Landsat Images and GIS." Computers and Electronics in Agriculture 37.1-3 (2002): 173-83. Web. 10 Oct. 2013.

Mockus, Victor. "Section 4 Hydrology, Chapter 21. Design Hydrographs." National Engineering Handbook Section 4, Hydrology. Springfield, VA: N.T.I.S., 1965, reprinted in 1972. N. page. Print.

Morland, Howard. "Memories of Reese T-38's." Reese AFB Undergraduate Pilot Training. N.p., June 2011. Web. 4 Nov. 2013.

Myers, James W. T-38 Forward Windshield Development and Performance Demonstration Report. Ohio: Wright Patterson Air Force Base, 1992. Print.

National Engineering Handbook: Part 630: Chapter 19, Transmission Losses. Washington, D.C.: U.S. Deptartment of Agriculture, Natural Resources Conservation Service, 2007. Web.

North State Resources, Inc. 2010. Surface Flow Study, Edwards Air Force Base. Prepared by North State Resources, Inc., Redding, California for Edwards Air Force Base and U.S. Army Corps of

Engineers, Sacramento District. U.S. Army Corps of Engineers Contract W91238-07- D-0022. February 2010.

NRCS, USDA. "Urban hydrology for small watersheds-Technical Release 55 (TR55)." (1986).

Oak Ridge National Laboratory Distributed Active Archive Center (ORNL DAAC). "Data Description." Daymet Data Description. n.d. Web. 20 Oct. 2013.

Prescott, Alan B., and Thomas U. Barkely. "Chapter 1 Approaches to Estimating the Depth and Duration of Playa Lake Floodig." Trends in Water Resources Research. New York, NY: Nova Science, 2008. N. pag. Print.

Römkens, M. J. M., et al. "Surface sealing and infiltration." Process studies in hillslope hydrology. (1990): 127-172.

Simley, J.D., Carswell Jr., W.J., 2009, The National Map—Hydrography: U.S. Geological Survey Fact Sheet 2009-3054, 4 p.

Singh, V. P. Rainfall-runoff Relationship. Littleton, CO: Water Resources Publications, 1982. Print.

Smith LM (2003) Playas of the Great Plains. University of Texas Press, Austin.

Snider, Dean. "Section 4 Hydrology, Chapter 16. Hydrographs." National Engineering Handbook. Springfield, VA: N.T.I.S., 1972. N. page. Print.

Squires, Gregory. Urban Sprawl: Causes, Consequences and Policy Responses. Washington: Urban Institute, 2002. Print.

Stuebe, Miki M., and Douglas M. Johnston. "Runoff Volume Estimation Using Gis Techniques." Journal of the American Water Resources Association 26.4 (1990): 611-20. Web. 11 Oct. 2013.

Tauer, W., and G. Humborg. Runoff Irrigation in the Sahel Zone: Remote Sensing and Geographical

    Information Systems for Determining Potential Sites. Ede, Netherlands: CTA, 1992. Print.

Thompson, Mark. "A Persistent (Feathered) Threat to U.S. Air Superiority | TIME.com." Swampland A

    Persistent Feathered Threat to US Air Superiority Comments. TIME, 4 Nov. 2013. Web. 08 Feb.

    2014.

Todini, E. "Rainfall-runoff modeling—Past, present and future." Journal of Hydrology 100.1 (1988): 341-

    352.

U.S. Environmental Protection Agency and U.S. Geological Survey. "NHDPlus Version 2 User Guide."

    Horizon Systems Corporation., 15 Jan. 2013. Web. 16 Oct. 2013.

U.S. Geological Survey and U.S. Department of Agriculture, Natural Resources Conservation Service,

    2012, Federal Standards and Procedures for the National Watershed Boundary Dataset (WBD)

    (3d ed.): U.S. Geological Survey Techniques and Methods 11–A3, 63 p., available only at

    http://pubs.usgs.gov/tm/tm11a3/.)

U.S. Geological Survey. "NHD User Guide." NHD User Guide. N.p., n.d. Web. 31 Oct. 2013.

University of California Cooperative Extension, California Department of Water Resources. "A Guide to

    Estimation Irrigation Water Needs of Landscape Plantings in California, The Landscape

    Coefficient Method and WUCOLS III." N.p., Aug. 2000. Web.

Yuan, F. "Land-cover Change and Environmental Impact Analysis in the Greater Mankato Area of

    Minnesota Using Remote Sensing and GIS Modeling." International Journal of Remote Sensing

    29.4 (2008): 1169-184. Web. 11 Sept. 2013.

Datasets Used

Coordinated effort between the United States Department of Agriculture-Natural Resources

Conservation Service (USDA-NRCS), the United States Geological Survey (USGS), and the United

States Environmental Protection Agency (US EPA). The Watershed Boundary Dataset (WBD) was

created from a variety of sources from each state and aggregated into a standard national layer

for use in strategic planning and accountability. Watershed Boundary Dataset for {Los Angeles,

California}, State [Online WWW]. Available URL: "http://datagateway.nrcs.usda.gov" [Accessed

2013]

Fry, J., Xian, G., Jin, S., Dewitz, J., Homer, C., Yang, L., Barnes, C., Herold, N., and Wickham, J., 2011.

Completion of the 2006 National Land Cover Database for the Conterminous United States,

PE&RS, Vol. 77(9):858-864.

Gesch, D.B., 2007, The National Elevation Dataset, in Maune, D., ed., Digital Elevation Model

Technologies and Applications: The DEM User's Manual, 2nd Edition: Bethesda, Maryland,

American Society for Photogrammetry and Remote Sensing, p. 99-118.

Gesch, D., Oimoen, M., Greenlee, S., Nelson, C., Steuck, M., and Tyler, D., 2002, The National

Elevation Dataset: Photogrammetric Engineering and Remote Sensing, v. 68, no. 1, p. 5-11.

NASA Landsat Program, 2003, Landsat ETM+, USGS, Sioux Falls, 1989-2012.

Surface weather on a 1 km grid for North America, 1980-2012. Acquired online

(http://daymet.ornl.gov/) from August 2013 through January 2014 from Oak Ridge National

Laboratory Distributed Active Archive Center, Oak Ridge, Tennessee, U.S.A.

http://doi:10.3334/ORNLDAAC/Daymet_V2

Thornton, PE, MM Thornton, BW Mayer, N Wilhelmi,Y Wei, RB Cook 2012. Daymet.

Appendix

Appendix A

Glossary of Terms

AMC	Antecedent Moisture Condition
Arc Hydro	Esri's Hydrologic Modeling Extension
ArcMap	A Geographical Information System Software
AVIRWMP	Antelope Valley Integrated Regional Water Management Plan
CN	Curve Number
Daymet	Spatially Referenced Meteorological Dataset
DEM	Digital Elevation Model
EAFB	Edwards Air Force Base
ESDIS	Earth Science Data and Information System
Esri	Supplier of GIS Software ArcMap
ETM	Enhanced Thematic Mapper
GCS	Geodetic Coordinate System
GIS	Geographical Information System
HEC-DSSVue	Hydrologic Engineering Centre - Data Storage System Visual Utility Engine
HEC-geoHMS	Hydrologic Engineering Centre - geoHydrologic Modeling System
HEC-HMS	Hydrologic Engineering Centre - Hydrologic Modeling System
LACSD	Los Angeles County Sanitation Districts
LAX	Los Angeles International Airport
LiDAR	Light and Radar; a remote sensing technology
LWRP	Lancaster Water Reclamation Plant
NASA	National Aeronautics and Space Administration
NCDC	National Climate Data Center
NED	National Elevation Dataset
NHDPlus	National Hydrography Database Plus
NLCD	National Land-cover Database
NRCS	Natural Resource Conservation Service
SNOTEL	SNOwpack and TELemetry
SSURGO	Soil Survey Geographic Database
US EPA	United States Environmental Protection Agency
USGS	United States Geological Survey
WBD	Watershed Boundary Dataset
WGS84	World Geodetic Coordinate System
FMD04	Flood Assessment for Rosamond Dry Lake, Edwards Air Force Base, California. French, Miller and Dettling circa 2004.
FM	Full Model
SM	Simplified Model

Software, Datasets and Technical Manuals

The model required the use of two software along with extensions developed primarily for the purpose of hydrologic modeling. Moreover, an assortment of free and readily available datasets were acquired to calculate various hydrological parameters for the. This section lists and describes the methods, software and datasets used to build the model. These descriptions provide the reader the purpose, source and a summarized technical specification of the dataset and the software. It is imperative to describe how these pieces cohere and supplement each other in order to understand the model.

ArcMap 10.0: ArcMap is geoprocessing software developed by Esri and comes bundled with their ArcGIS software suite. ArcMap is the principal software of the ArcGIS suite and its main function is digital cartography. It allows users to create, manipulate and publish geospatial datasets. Relevant to this study, it can represent geographic and hydrological information as a collection of layers and features. Additional ArcGIS package extensions provide a versatile set of tools capable of performing a slew of operations including, but not limited to watershed delineation, areal analysis, volume calculation et cetera.

Arc Hydro: Arc Hydro is a geospatial hydrology toolset for ArcMap and comes free with an ArcGIS license. It consists of two main components: Data Model and Tools. The data model contains five principle water resources feature categories: network, drainage, channels, hydrography and time series. It also contains utilities that enable users to manipulate the parameters in the data model while providing functions that are essential for hydrologic analyses including watershed delineation from a DEM, batch-point sub-basin generation, flow path tracing et cetera.

HEC-geoHMS: Similar to Arc Hydro Tools, HEC-geoHMS is another free geospatial hydrology toolset for use in ArcMap. It is capable of performing terrain and basin performing operations similar to Arc Hydro. Its main purpose, however, lies its ability to bridge the gap between the grid-based modeling facilitated by the advent of GIS and the traditional use of averaged parameters. In this project, it was mainly used to develop hydrologic modeling parameters for HEC-HMS including CNs, lag time, river length, and centroid elevation.

HEC-HMS: HEC-HMS is free hydrologic modeling software developed by the Hydrologic Engineering Center of the Army Corps of Engineers. The heart of the software is its ability to separate the water cycle into manageable mathematical models to simulate the precipitation and runoff in a variety of dendritic watersheds. The resulting hydrograph can be used to analyze and predict runoff and water availability. It also allows users to insert anthropogenic structures like artificial reservoirs and sinks into the model. It boasts an array of tools common in the field of hydrologic engineering. This enables the end-user to use the software in a wide range of situations.

HEC-DSSVue: The input and output of HEC-HMS are stored in .dss files. HEC-DSSVue is a java based free utility that allows the user to open and manipulate these files. It allows users to create tables and graphs and also incorporates many mathematical functions. But most important of all, it can export the data to a Microsoft Excel spreadsheet.

Soil Survey Geographic (SSURGO): SSURGO dataset is the digitized form of soils data collected by the NRCS over the course of the century. Surveyors were sent out to collect samples, which were later analyzed in laboratories. SSURGO dataset consists of maps that are linked to a database via a common parameter and a text file explaining the nature of the data and metadata. The database contains information about the soils. SSURGO data can be acquired for free and is in the 1984 revision of world geodetic coordinate system (WGS84).

National Land Cover Database 2006 (NLCD2006): NLCD2006 is land cover data based on the Landsat Enhanced Thematic Mapper+ (ETM+) circa 2006 satellite data. It has a spatial resolution of 30 meters and categorizes land cover into sixteen different classes. It can be acquired for free from the Multi-Resolution Land Characteristics Consortium (MRLC) website. Maps for percent developed impervious surface and land cover were retrieved from this dataset.

National Elevation Dataset (NED): NED is a dataset that contains a three dimensional representation of the earth's terrain provided by the USGS. The dataset is built using USGS topography maps and remote sensing techniques such as Light Detection and Ranging (LiDAR) and digital photogrammetry. The best resolution available at the time of writing for the research area was 1/3 arc seconds (about 10 meters or 32.8 feet). NED is distributed in geographical co-ordinates and is available for free.

National Hydrography Database Plus (NHDPlus) Version 2: Envisioned by the US EPA Office of Water, NHHDPlus is a hydrologic database developed by Horizon Systems Corporation with assistance from the USGS. The continental U.S. is divided into 21 drainage areas and the dataset incorporates features from the National Hydrography Dataset (NHD), the National Elevation Dataset (NED), and the Watershed Boundary Dataset (WBD). Consequently, it contains a plethora of application-ready hydrologic grids and features including catchment polygons, stream network, drainage area characteristics, flow direction, flow direction grids, elevation, slope, volume and velocity estimates of flow lines et cetera. In this study, only the stream network and the watershed boundary were used.

The stream network in NHDPlus, a spatially referenced set of linear features linking to form a flow nexus/structure, is from the National Hydrography Dataset [medium resolution, ~1 inch of Map =100,000 in reality (1:100K scale)]. The medium resolution NHD was originally built from the USGS Quad maps. For the purposes of NHDPlus, the NHD was corrected and updated where errors or omissions were detected.

Watershed Boundary Dataset (WBD): The watershed boundary included in NHDPlus2 is derived from WBD. The dataset divides drainage areas based on Hydrologic Unit (HU). The *Federal Standard for Delineation of Hydrologic Unit Boundaries* provides the following definition,

> A hydrologic unit is a drainage area delineated to nest in a multi-level, hierarchical drainage system. Its boundaries are defined by hydrographic and topographic criteria that delineate an area of land upstream from a specific point on a river, stream or similar surface waters. A hydrologic unit can accept surface water directly from upstream drainage areas, and indirectly from associated surface areas such as remnant, non-contributing, and diversions to form a drainage area with single or multiple outlet points.

The techniques, criteria and standards for the delineation of HUs are set on a federal level by the U.S Department of the Interior and the USGS. The dataset comes in various nested resolutions: the coarsest, a two-digit HU, divides continental US into 22 regions while the finest, a twelve digit HU, contains 97,442 sub-basins. For the purpose of this research, the ten-digit HU was used; it divides the US into 17828 watersheds.

Daymet: Part of NASA's Earth Science Data and Information System (ESDIS) Project, Daymet implements a collection of software and algorithms to iteratively interpolate and extrapolate from spatially referenced precipitation observations of meteorological data to produce gridded estimates. The spatially referenced data are procured from ground surface observation stations managed by National Climate Data Center (NCDC) and NRCS's SNOwpack and TELemetry (SNOTEL).

The data are provided at a 1km spatial resolution and consist of daily values for maximum and minimum temperatures, precipitation, shortwave radiation, vapor pressure, snow-water equivalent and day length. The dataset divides continental U.S into a system of 2 degree x 2 degree squares. Gridded data for each square are calculated based on ground observations from that square as well as the eight surrounding squares. The data can be downloaded for free from their website.

Landsat: The Landsat Program, a joint venture of the Department of the Interior, NASA, and the Department of Agriculture, provides a collection of remotely sensed images of the earth surface. These images are stored in the USGS archive and are available for free. The first Landsat satellite was launched on 23rd July, 1972. Landsat satellites complete one revolution in sixteen days. There are two operational satellites as of February 2014. Landsat images were used to estimate the volume of water in RDL due the lack of gauged data. The volume was extrapolated from an area-volume table created by Simone Evett. Values for inundated areas were estimated from the Landsat images and the corresponding volume was calculated from the LiDAR map of Rosamond Lake. The detailed table can be found in the appendix c).

The following technical manuals were also consulted during this study:

- Urban Hydrology for Small Watersheds (TR-55): Released in 1986 by the NRCS, this documents is a revised version of a manual released by the SCS in 1975. It contains a detailed description of various methods to "calculate storm runoff volume, peak rate of discharge, hydrographs, and storage volumes required for floodwater reservoirs" applicable for small, urban, watersheds (Cronshey et al. 1975). Chapter 2 (Estimating Runoff) of TR-55 explains the NRCS-CN approach for calculating storm runoff. Relevant equations, graphs, look-up tables and examples are available. For the purposes of this research, Chapter 2 in TR-55 was extensively utilized.
- LA County Hydrology Manual: Developed by the LA County Department of Public Works and released in 2006, this document contains design procedures and techniques for calculating storm runoff in LA County. Since the watershed modeled in this study experiences similar climatic conditions to LA County, the unit hyetograph developed in this document was used to temporally distribute the spatially-varying historical and derived (elevation-based) storms used in this study.

- <u>A Guide to Estimating Irrigation Water Needs of Landscape Plantings in California</u>: Published by the University of California Cooperative Extension and California Department of Water Resources in 2000, this document contains information regarding irrigation water needs and water use classification in California. This documents was exclusively used to estimate the daily evapotranspiration for the watershed draining into RDL.
- <u>Lancaster General Plan 2030</u>: Published in 2009, this document contains future plans for various aspects, including zoning and development, of the city of Lancaster until the year 2030. Since the impact of urbanization on runoff is modeled in this study, this document was consulted to identify and replicate the trend in urbanization. The city has chosen to develop the undeveloped areas within the city.

Appendix B

<u>Watershed Delineation</u>

Delineating a watershed is paramount to hydrologic modeling. In order to delineate a dendritic terrain whose stream network is known, follow the following process. Until the advent of GIS, watersheds were delineated by hand with the use of topographic maps. Watershed delineation in GIS is referred to as terrain processing. There are various approaches to processing a terrain in GIS, following are the steps to process a dendritic terrain whose stream network is known/available as implemented in this study.

Requirements

<u>Software:</u> ArcGIS and Arc Hydro tools
<u>Datasets:</u> DEM and Stream Network. There are two different approaches to acquiring this data. The DEM, which is part of the NED and the Stream network which is part of NHD can be acquired from USGS's National Map Viewer and Download Platform here: http://nationalmap.gov/viewer.html

The easier way to acquire both these data is by downloading the NHDPlus version 2 dataset from here: http://www.horizon-systems.com/nhdplus/. NHDPlus comes with all the datasets necessary for terrain processing including flow direction and flow accumulation calculated based on hydro enforced terrain (using NHD 100k). However, it is coarser resolution, 30 meters, data compared to the NED which gets updated every 3-4 months.

After the data is downloaded, one can proceed further.

If the Arc Hydro tools toolbar is not visible, it can be added to the map document by, following is a picture of the Arc Hydro Tools Toolbar. Load the DEM and the Stream Network and save the project in a new folder.

<u>1 Fill Sinks</u>
The first step in processing a terrain is filling the sinks. Sometimes DEM contains cells that do not contain a drainage direction, i.e., the cells surrounding them have higher elevations so water ponds in the sink. Filling sinks looks for these imperfections and adjusts the elevation of such cells by referring to the cells surrounding the cell. It is advised not to change the output file names from what is suggested by the program. The command can be accessed on the Arc Hydro Toolbar: Terrain Preprocessing\Fill Sinks

<u>2 DEM Reconditioning</u>
DEM reconditioning allows one to impress the stream network onto the DEM. This is also known as burning. Using the same tool to impress the watershed boundary on the DEM is called fencing. Reconditioning adjusts the DEM to match the surface elevation with vector data (stream network, watershed boundary). To execute this function the filled DEM (Fil1) is needed along with the stream network/watershed boundary. Following are the suggested parameter values for DEM reconditioning:

Stream Buffer: 5
Smooth Drop/Raise: 10
Sharp Drop/Raise: 100
These values can be tinkered with to suit the needs of the user.

Access: Terrain Preprocessing\DEM Reconditioning

After reconditioning the DEM, fill the sinks to rid the DEM of the sinks introduced by DEM Reconditioning.

3 Flow Direction
Flow direction computes the direction of flow for a given grid. It is represented by integers. Following is the numerical representation of flow direction in ArcMap:

Table A 1: ArcMap Flow Direction Legend

32	64	128
16		1
8	4	2

For instance, a value of 4 denotes flow directed completely downwards. Following is an illustration of a flow direction grid (Flow_Dir) derived from a DEM (Elev_Ras).

Elev_Ras   =   Flow_Dir

Figure A 1: Flow Direction Raster based on DEM. Source: http://help.arcgis.com

The parameters for flow direction are as follows:
Hydro DEM: Fil (Filled, Reconditioned DEM)
Outer Wall Polygon: Null
Flow Direction Grid: Fdr

Access: Terrain Preprocessing\Flow Direction

4 Flow Accumulation

Flow accumulation is a grid derived from flow direction. It is accumulated flow to individual cells. The following diagram illustrate how it functions:
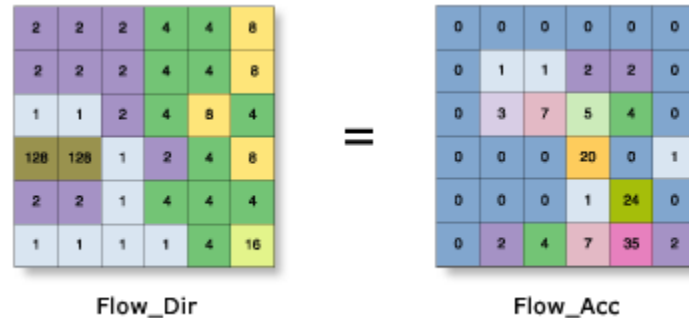
Figure A 2: Flow Accumulation Grid based on Flow Direction Grid. Source: http://help.arcgis.com

The parameters for flow direction are as follows:
Flow Direction Grid: Fdr
Flow Accumulation Grid: Fac

Access: Terrain Preprocessing\Flow Accumulation

5 Stream Definition

This function simulates streams based on the flow accumulation grid. The stream grid contains "1"for values in the flow accumulation grid that exceed the threshold number of cells and no values otherwise. The parameters for stream definition are as follows:
Flow Accumulation Grid: Fac
Number of Cells: Dependent on Area
Area (square km): 15 (this value can be adjusted to the needs of the project)
Stream Grid: Str

Access: Terrain Preprocessing\Stream Processing

6 Stream Segmentation

This function basically separates and groups the streams. It assigns uniquely identical values to cells comprising the same stream segment. The parameters for stream definition are as follows:
Flow Accumulation Grid: Fac
Stream Grid: Str
Sink Watershed Grid: Null
Sink Link Grid: Null
Stream Link Grid: StrLnk

Access: Terrain Preprocessing\Stream Segmentation

7 Catchment Grid Delineation

This function creates catchments based on the stream segment that drains to an area. It assigns

uniquely identical values to cells comprising the same catchment. The parameters for stream definition are as follows:

Flow Direction Grid: Fdr
Link Grid: StrLnk
Catchment Grid: Cat

The two upcoming function basically convert Raster Data to Vector data. In simpler terms, these function convert our grid (raster) to lines and shapes (Vector). A single grid in a raster represents a point in a vector, a series of grid represent lines while a zone of grid represent polygons.

Catchment Polygon Processing: Uses *Catchment Grid* to generate Polygons vector data. Parameters are:
Catchment Grid: Cat
Catchment: Catchment

Access: Terrain Preprocessing\Catchment Polygon Processing.

8 Drainage Line Processing: Uses *Stream Link* Grid to generate Drainage Line vector data. Parameters are:

Stream Link Grid: StrLnk
Flow Direction Grid: Fdr
Drainage Line: DrainageLine

Access: Terrain Preprocessing\Drainage Line Processing

9 Adjoint Catchment Processing: Uses Catchment vector to generate accumulated catchments. Polygons representing the upstream drainage area and outlet points are constructed and stored here. Parameters are:

Drainage Line: DrainageLine
Catchment: Catchment
Adjoint Catchment: AdjointCatchment

Access: Terrain Preprocessing\Adjoint Catchment Processing

10 Drainage Point Processing: This function generate drainage points for the catchments. Parameters are:

Flow Accumulation Grid: Fac
Catchment Grid: Cat
Catchment: Catchment
Drainage Point: DrainagePoint

Access: Terrain Preprocessing\ Drainage Point Processing

11 Batch Watershed Delineation: This function generates a watershed based on an input point. To perform batch watershed delineation, select Batch Point Generation tool and click on the drainage point that drains into the polygon which happens to be the watersheds outlet. A window will ask confirmation for the name of the batch point, once you select *OK*, a point is created and a form displaying the point definition is displayed. Enter the following parameters:

Name: Rosamond (name of watershed)
Description: Any description
BatchDone: 0 (0 indicates that the watershed delineation hasn't been performed)
SnapOn: 1
Type: Outlet

Click OK

To delineate watershed based on the batch point select *Watershed Processing\Batch Watershed Delineation.* A delineated watershed along with the outlet point will appear.

This completes the watershed delineation process.
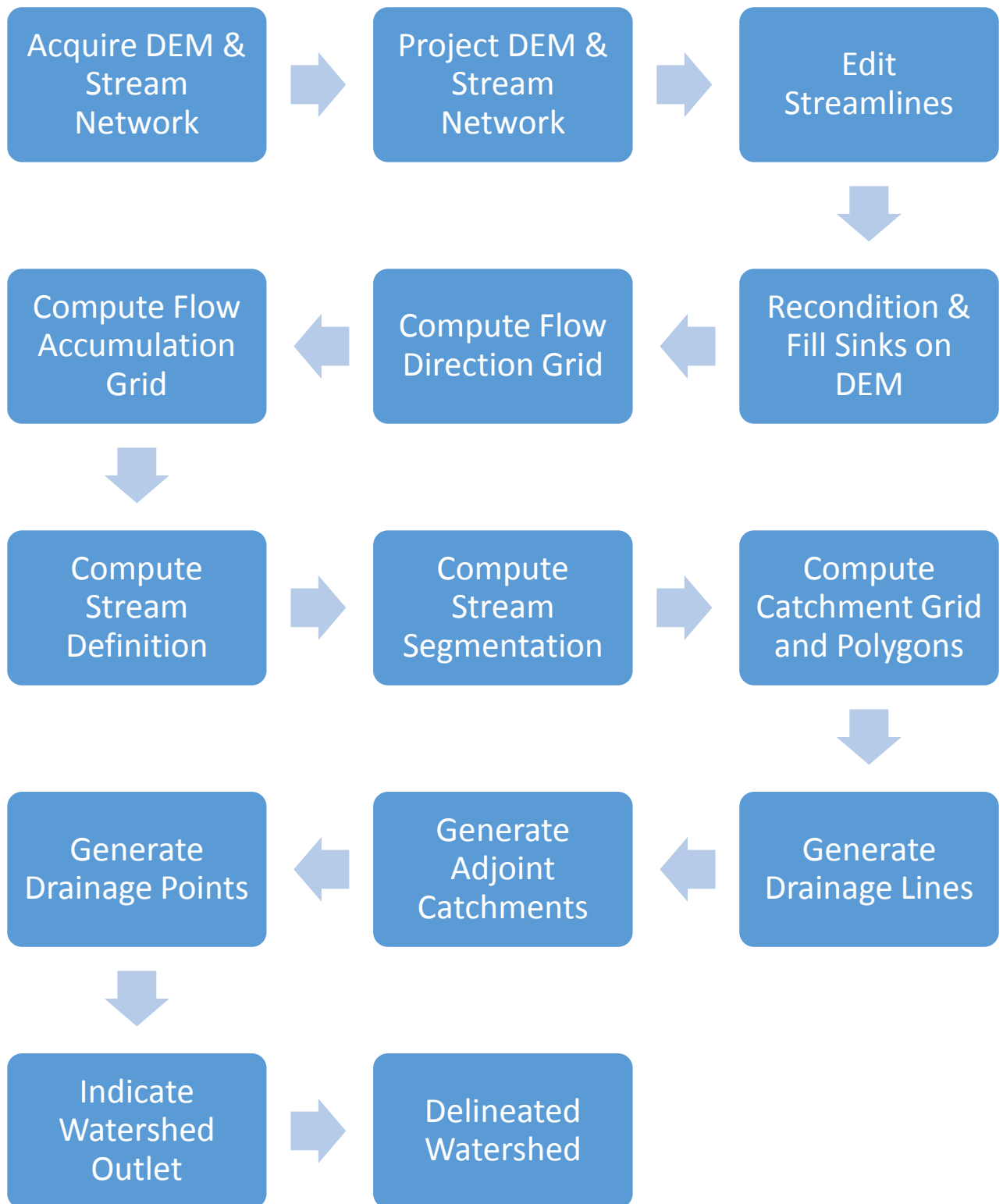
Figure 16: Process Diagram to Delineate a Watershed in ArcMap.

CN Grid

Creating a curve number grid is somewhat complex, tedious and time consuming process that requires intermediate knowledge of ArcMap, Microsoft Access, HEC-geoHMS, SSURGO dataset and NLCD dataset along with their metadata. A basic structure of the method is included below:

DEM, Soil and Land-cover Data

Project All Datasets

Link Metadata to Maps

Merge Soil and Land-cover Data

Create CN Look-up Table

Process CN Grid
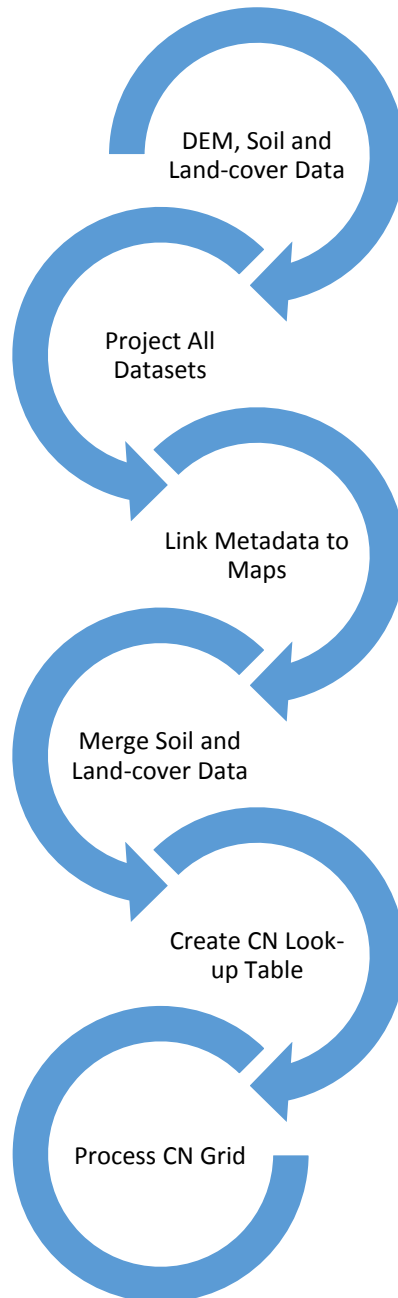
Figure 17: Process Diagram for Creating a Curve Number Grid in GIS.

Exporting the model to HEC-HMS using HEC-geoHMS

The user manual for HEC-geoHMS includes an example for creating a HEC-HMS model from a watershed delineate in GIS. The HEC-HMS model for this project was created by carrying out the processes from the same example, but with different data.

Data Manipulation

Throughout the process of this study, some datasets were manipulated. The nature of and reasoning behind these manipulations are listed below in chronological order:

- Data Projection: All downloaded data were in geographic coordinates; a spherical coordinate system where a point is located using angles and radial distance. Moreover, unlike planar systems, spherical systems have consistent lengths only at the center, i.e., the length of the latitude and longitude is equal at the equator only. "Projecting" converts the dataset from spherical to a Cartesian coordinate (planar) system without distorting the data. It also enables a linear system of measurement. The data were projected to Universal Transverse Mercator coordinate system for zone 11.
- Editing Streamlines: Rosamond Lake is the eventual destination for all runoff and there are multiple streamlines flowing into it. This would require setting-up and running individual models for each discharge point (streamline). To keep things simple, it was assumed that the lake, a sink, did not exist, and combined all the streamlines into one and extended it to go out of the lake, thus creating a single-point discharge. Moreover, it is known that Piute ponds were flowing into the lake but the streamlines suggested otherwise, the streamlines were adjusted to include flow from Piute Ponds to Rosamond Lake.
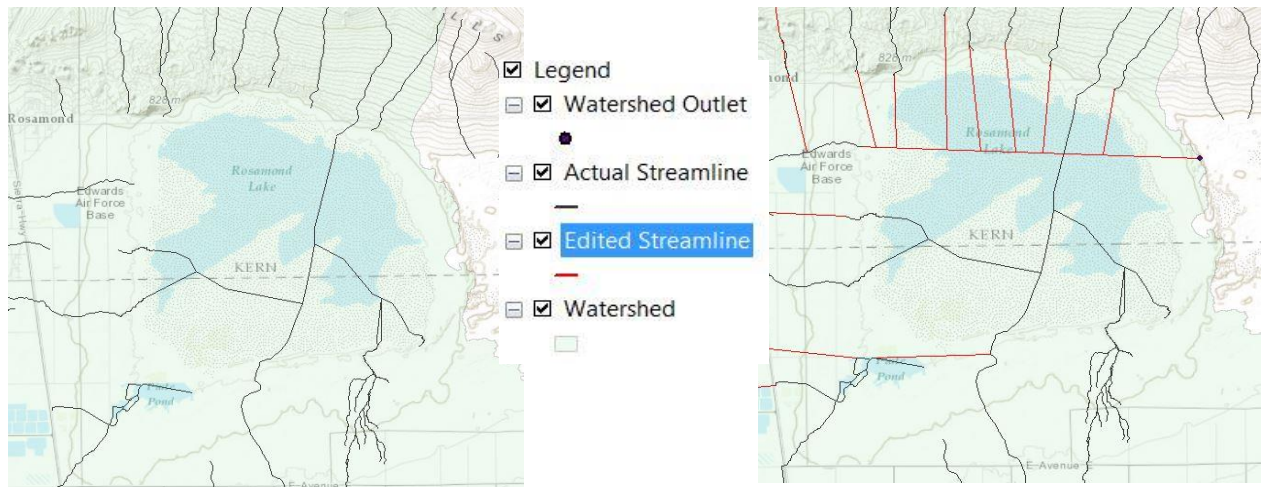
Figure A 3: Actual Streamlines (Left), Edited Streamlines with Outlet (Right)

- DEM Reconditioning: In order to simulate flow patterns based on the streamlines, the streamlines were burned into the DEM. This imposes the features of the streamlines into the DEM by dropping the Z-coordinate (depth) in the DEM. The software allows the user to set the magnitude for the drop.

- Empty Soil Codes: There were random "holes" in the SSURGO soil map where polygon(s) were assigned a null value for the hydrologic soil group. Since this parameter is essential in calculating the curve number, the null values were "manually-interpolated" by referring to the surrounding polygons and replacing the missing value with what was deemed reasonable. The soil map had over three hundred thousand polygons out of which over seven thousand were had nulls for the hydrologic soil group. Simone Evett, an undergraduate student at Loyola Marymount University, did most of the manual-interpolation.
- Curve Number Lookup Table: A lookup table was needed to calculate the curve number based on the land cover and soil group. The following table, based on the information found on the land cover legend (http://www.mrlc.gov/nlcd06_leg.php) and curve number lookup table found in the USDA's "Urban Hydrology for Small Watersheds Technical release 55", was created:

Table A 2: Curve Number Lookup table for this study.

Land Use Value	Description	Curve Number for Hydrologic Soil Group			
		A	B	C	D
11	Open Water	100	100	100	100
21	Developed, Open Space (Impr %<20)	39	61	74	80
22	Developed, Low Intensity (20 < Impr% < 49)	49	69	79	84
23	Developed, Medium Intensity (50 < Impr% < 79)	68	79	86	89
24	Developed, High Intensity (80 < Impr% < 100)	91	94	95	96
31	Bare Land	77	86	91	94
41	Deciduous Forest (Fair)	36	60	73	79
42	Evergreen Forest (Good)	30	55	70	77
43	Mixed Forest (Fair)	43	65	76	82
52	Shrub/Scrub (Fair)	49	69	79	84
71	Grasslands/Herbaceous	49	69	79	84
81	Pasture/Hay (Fair)	68	71	81	89
82	Row Crops	70	79	84	88
90	Woody Wetlands	98	98	98	98
95	Emergent Herbaceous Wetlands	98	98	98	98

Appendix C

Appendix C

Parameter Lists

Table A 3: List of sub-basin parameters

Parameter
Unique Identification Number
Name
Length (ft)
Area (ft^2)
Slope
Centroid Elevation (ft)
Precipitation Gage
Total Storm Depth (in)
Loss Method
Transmission Method
Percent Impervious Surface Area
Initial Abstractions (in)
Curve Number
Lag Method
Lag Time

Table A 4: List of river parameters

Parameter
Unique Identification Number
Name
Length (ft)
Slope
Elevation Upstream
Elevation Downstream
Routing Method

Look-up Tables and Graphs

Table A 5: Fractional transmission loss coefficients for runoff reduction (Mockus, 1972).

Drainage Area (mi^2)	Climatic Index						
	1.0	0.9	0.8	0.7	0.6	0.5	≤0.4
≤1	1.00	1.00	1.00	1.00	1.00	1.00	1.00
2	1.00	0.98	0.97	0.95	0.93	0.90	0.87
3	1.00	0.98	0.95	0.92	0.89	0.85	0.80
4	1.00	0.97	0.94	0.90	0.86	0.81	0.76
5	1.00	0.96	0.92	0.88	0.84	0.78	0.73
6	1.00	0.96	0.92	0.87	0.82	0.76	0.70
7	1.00	0.96	0.91	0.86	0.81	0.75	0.68
8	1.00	0.95	0.90	0.85	0.79	0.73	0.66
9	1.00	0.95	0.90	0.84	0.78	0.72	0.65
10	1.00	0.95	0.89	0.84	0.77	0.71	0.63
20	1.00	0.93	0.86	0.79	0.72	0.64	0.55
30	1.00	0.93	0.85	0.77	0.69	0.60	0.51
40	1.00	0.92	0.84	0.75	0.66	0.57	0.48
50	1.00	0.91	0.83	0.74	0.65	0.55	0.46
60	1.00	0.91	0.82	0.73	0.63	0.54	0.44
70	1.00	0.91	0.81	0.72	0.62	0.53	0.43
80	1.00	0.90	0.81	0.71	0.62	0.52	0.42
90	1.00	0.90	0.80	0.71	0.61	0.51	0.41
100	1.00	0.90	0.80	0.70	0.60	0.50	0.40
150	1.00	0.89	0.78	0.68	0.57	0.47	0.37
200	1.00	0.89	0.77	0.66	0.56	0.45	0.35
250	1.00	0.88	0.77	0.65	0.54	0.44	0.33
300	1.00	0.88	0.76	0.64	0.53	0.42	0.32
350	1.00	0.87	0.75	0.64	0.52	0.41	0.32
400	1.00	0.87	0.75	0.63	0.51	0.41	0.30
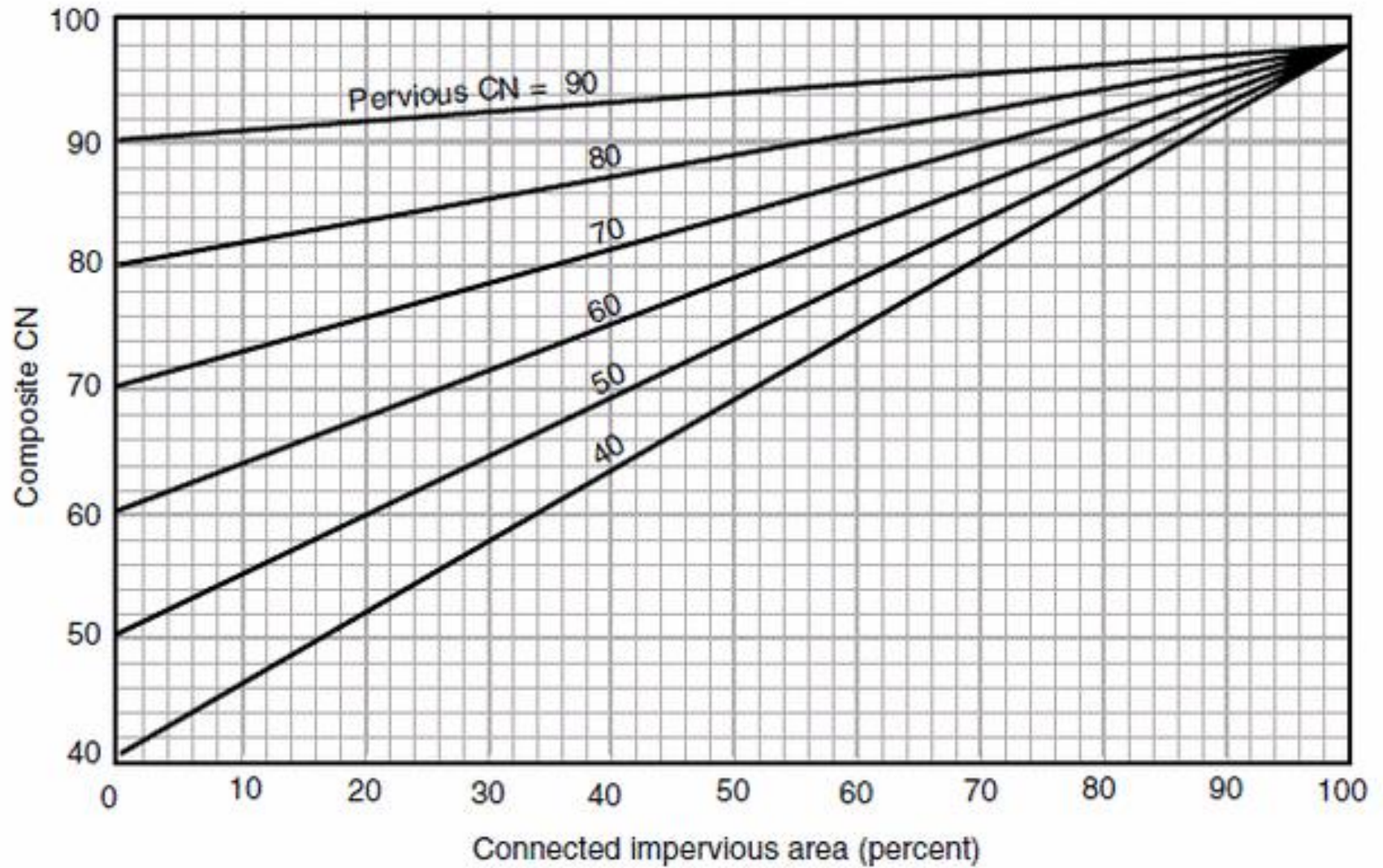
Figure A 4: Composite curve number and impervious area graph (TR-55, 1986).

Table A 6: Area-volume relationship for Rosamond Dry Lake (Evett, Unpublished)

Elevation (m)	Area (m^2)	Volume (m^3)	Volume (ac-ft)	Avg Depth (m)
692.1	0	0	0	0
692.2	3.61E-01	6.97E-03	5.65E-06	1.93E-02
692.3	8.86E+00	2.98E-01	2.42E-04	3.37E-02
692.4	8.22E+01	3.74E+00	3.04E-03	4.56E-02
692.5	5.10E+02	2.70E+01	2.19E-02	5.29E-02
692.6	3.73E+03	1.81E+02	1.47E-01	4.86E-02
692.7	2.22E+04	1.23E+03	1.00E+00	5.56E-02
692.8	2.33E+05	6.76E+03	5.48E+00	2.90E-02
692.9	4.74E+06	1.88E+05	1.52E+02	3.97E-02
693	1.89E+07	1.35E+06	1.09E+03	7.15E-02
693.1	2.95E+07	3.79E+06	3.07E+03	1.28E-01
693.2	3.51E+07	7.04E+06	5.71E+03	2.01E-01
693.3	4.14E+07	1.09E+07	8.80E+03	2.62E-01
693.4	4.54E+07	1.52E+07	1.23E+04	3.35E-01
693.5	4.86E+07	1.99E+07	1.61E+04	4.10E-01
693.6	5.07E+07	2.49E+07	2.02E+04	4.90E-01
693.7	5.27E+07	3.01E+07	2.44E+04	5.70E-01
693.8	5.42E+07	3.54E+07	2.87E+04	6.53E-01
693.9	5.55E+07	4.09E+07	3.31E+04	7.37E-01
694	5.67E+07	4.65E+07	3.77E+04	8.20E-01
694.1	5.78E+07	5.22E+07	4.23E+04	9.03E-01
694.2	5.87E+07	5.80E+07	4.71E+04	9.88E-01
694.3	5.96E+07	6.40E+07	5.19E+04	1.07E+00
694.4	6.02E+07	6.99E+07	5.67E+04	1.16E+00
694.5	6.10E+07	7.60E+07	6.16E+04	1.25E+00
694.6	6.16E+07	8.21E+07	6.66E+04	1.33E+00
694.7	6.23E+07	8.83E+07	7.16E+04	1.42E+00
694.8	6.29E+07	9.46E+07	7.67E+04	1.50E+00
694.9	6.36E+07	1.01E+08	8.18E+04	1.59E+00
695	6.42E+07	1.07E+08	8.70E+04	1.67E+00
695.1	6.48E+07	1.14E+08	9.22E+04	1.75E+00

Variable Manipulation Tables

Table A 7: Original and manipulated curve number and percentage of impervious surface area for various levels of infill urbanization

Sub-basin	Area(mi^2)	PctImp	CN	25% Increase in PctImp		50% Increase in PctImp		100% Increase in PctImp	
				CN	PctImp	CN	PctImp	CN	PctImp
W2030	14	2	77	78	3	79	3	80	4
W2100	13	3	85	86	4	88	4	91	6
W2110	17	0.5	81	81	0.6	81	0.7	82	1
W2160	6	34	68	80	43	88	51	95	69
W2210	13	4	76	77	4	79	5	81	7
W2220	5	30	69	80	38	88	45	94	61
W2230	22	12	64	70	15	77	18	83	24
W2240	9	22	72	78	28	86	34	91	45
W2250	25	21	68	75	26	84	31	90	41
W2270	5	0.2	75	76	0.2	76	0.3	76	0.4
W2280	8	18	71	77	23	83	27	87	36
W2300	10	0.9	73	74	1	74	1	75	2
W2310	5	4	68	70	5	72	6	73	9
W2320	8	6	66	69	7	72	9	74	11
W2350	6	9	61	65	12	69	14	75	19
W2360	19	21	70	78	27	84	32	90	43
W2370	9	1	59	60	2	62	2	63	3
W2430	8	1	75	76	1	76	2	78	2

Table A 8: Fractional transmission loss coefficient manipulation.

River	Fractional Transmission Loss Coefficient	61% of FTLC
R1030	0.74	0.71
R1050	0.59	0.77
R1070	0.65	0.75
R110	0.77	0.70
R1110	0.53	0.79
R1130	0.53	0.79
R1160	0.70	0.73
R1180	0.69	0.73
R1190	0.60	0.76
R120	0.74	0.71
R1220	0.60	0.76
R1230	0.76	0.70
R1260	0.83	0.68
R130	0.67	0.74
R140	0.67	0.74
R160	0.79	0.69
R170	0.69	0.73
R180	0.74	0.71
R240	0.74	0.71
R250	0.53	0.79
R260	0.74	0.71
R270	0.64	0.75
R280	0.67	0.74
R300	0.59	0.77
R320	0.61	0.76
R370	0.73	0.71
R390	0.78	0.69
R400	0.78	0.69
R410	0.71	0.72
R430	0.66	0.74
R440	0.78	0.69

R450	0.59	0.77
R460	0.59	0.77
R480	0.67	0.74
R510	0.66	0.74
R520	0.57	0.78
R540	0.58	0.77
R550	0.59	0.77
R560	0.63	0.75
R570	0.56	0.78
R580	0.71	0.72
R590	0.71	0.72
R600	0.59	0.77
R620	0.59	0.77
R640	0.59	0.77
R660	0.60	0.76
R670	0.61	0.76
R680	0.60	0.77
R700	0.66	0.74
R720	0.66	0.74
R760	0.57	0.78
R780	0.58	0.77
R820	0.60	0.76
R840	0.59	0.77
R860	0.72	0.72
R880	0.72	0.72
R90	0.56	0.78
R900	0.60	0.76
R910	0.67	0.74
R930	0.62	0.76
R940	0.72	0.72
R960	0.67	0.74
R970	0.60	0.76

Summary Tables

Table A 9: Replication of FMD04, table 10

Lower Elevation (ft)	Upper Elevation (ft)	Area (mi²)	CN	Th. Depth of Precip, Ia (in)	Precip, P (in)	Net Excess Precipitation, Q (in)	Net Runoff (ft-mi²)	CLRF	Cumulative runoff (ft-mi²)
7000	8200	6.4	71	0.82	19.97	19.16	10.2	1.00	10.2
5000	7000	81	71	0.82	15.01	14.20	95.8	0.71	75.3
4200	5000	83	82	0.44	10.67	10.23	70.8	0.47	68.7
3000	4200	348	51	1.92	7.57	5.65	163.9	0.31	72.1
2000	3000	686	76	0.63	4.16	3.53	201.9	0.30	82.2
	Lakebed	20		0	3.55	3.55	5.9	1.00	88.1
Total		1224.4					548.6		396.6

Table A 10: Simplified model without retention (similar to FMD04, table 10)

Average Elevation (ft)	Area (mi²)	CN	Th. Depth of Precip, Ia (in	Precip, P (in)	Net Excess Precipitation, Q (in)	Net Runoff (ft-mi²)	CLRF	Cumulative runoff (ft-mi²)
5348	31.1	75.5	0.65	15.0	14.4	37.3	0.71	37.3
4523	63.2	71.6	0.79	11.3	10.5	55.3	0.47	43.5
3532	431.2	71.8	0.78	7.9	7.1	254.6	0.31	92.4
2563	672.9	71.9	0.78	4.5	3.7	207.0	0.30	89.8
Total	1198.4					554.2		263.0

Table A 11: FMD04, table 10 with soil retention added.

Lower Elevation (ft)	Upper Elevation (ft)	Area (mi²)	CN	Retention, S (in)	Th. Depth of Precip, Ia (in)	Design Storm Precip, P (in)	Net Excess Precipitation, Q (in	Net Runoff (ft-mi²)	CLRF	Cumulative runoff (ft-mi²)
7000	8200	6.4	71	4.08	0.82	19.97	15.8	8.4	1.0	8.4
5000	7000	81	71	4.08	0.82	15.01	11.0	74.4	0.7	58.8
4200	5000	83	82	2.20	0.44	10.67	8.4	58.3	0.5	55.1
3000	4200	348	51	9.61	1.92	7.57	2.1	60.7	0.3	35.9
2000	3000	686	76	3.16	0.63	4.16	1.9	106.6	0.3	42.8
	Lakebed	20			0	3.55	3.6	5.9	1.0	48.7
Total		1224.4						314.4		249.6

Table A 12: Simplified model with soil retention.

Average Elevation (ft)	Area	CN	Retention (S)	Th. Depth of Precip (Ia)	Design Storm Precip (P)	Net Excess Precipitation (Q)	Net Runoff	CLRF	Cumulative Runoff
5348	31.1	75.5	3.24	0.65	15.0	11.7	30.4	0.71	30.4
4523	63.2	71.6	3.97	0.79	11.3	7.6	40.2	0.47	33.2
3532	431.2	71.8	3.92	0.78	7.9	4.6	163.9	0.31	61.1
2563	672.9	71.9	3.90	0.78	4.5	1.8	100.6	0.30	48.5
Total	1198.38						335.1		173.2

Simplified Model with Soil Retention

Table A 13: Runoff for various values of FTLC

Date	Landsat	Runoff		
		88% of FTLC	61% of FTLC (Model)	50% of FTLC
Dec-91	3,300	12,500	3,200	2,000
Feb-96	3,000	9,300	2,700	1,500
Jan-08	4,100	22,600	6,000	3,900
Feb-09	1,800	1,700	900	600

Table A 14: Landsat-based runoff volume estimation for historical storms

1	2	3	4	5	6	7	8	9
Start	End	Precipitation (in.)	Lapse (days)	Initial Area (mi^2)	Initial Volume (ac-ft)	Final Area (mi^2)	Final Volume (ac-ft)	Runoff Volume (ac-ft)
27-Dec-91	12-Jan-92	4.0	4	0	0	11.6	3,400	3,400
27-Nov-92	13-Dec-92	2.9	1	0	0	9.5	2,100	2,100
8-Feb-96	24-Feb-96	2.6	2	2.1	200	11.5	3,200	3,000
25-Nov-97	11-Dec-97	4.1	3	0	0	15.7	8,400	8,400
28-Jan-98	13-Feb-98	5.6	4	6.1	900	15.6	8,300	7,400
21-Jan-04	6-Feb-04	0.9	2	2.8	300	8.1	1,500	1,200
14-Dec-04	30-Dec-04	4.2	0	2.4	200	17.0	11,500	11,300
16-Jan-08	1-Feb-08	4.6	3	3.1	400	12.6	4,500	4,100
3-Feb-09	11-Feb-09	1.6	3	7.6	1,300	10.7	2,800	1,500
11-Feb-09	19-Feb-09	0.8	2	10.7	2,800	11.3	3,000	200
7-Dec-10	23-Dec-10	5.3	0	0	10	17.3	13,300	13,300

Table A 15: Runoff volume calculation for historical storms (performance test for the full model).

| Date | Precipitation (in) | Cumulative Precipitation, Pacc (in) | Detention Basins | | Landsat (ac-ft) | Daymet | | | AMC | Best Guess (ac-ft) | Lapse (days) |
			Lancaster (ac-ft)	Palmdale (ac-ft)		Dry (ac-ft)	Normal (ac-ft)	Wet (ac-ft)			
	0.00	0.00									
28-Dec-91	0.48	0.48	75	103		60	-	-	Dry	60	
29-Dec-91	0.75	1.23	157	222		79	-	-	Dry	79	
30-Dec-91	0.50	1.73	214	324		-	-	413	Wet	413	
3-Jan-92	0.31	1.92	247	391		-	-	117	Wet	117	
5-Jan-92	0.84	2.72	372	623		-	-	1184	Wet	1184	
6-Jan-92	0.33	3.05	426	666		-	-	88	Wet	88	
7-Jan-92	0.33	3.38	503	713		-	-	145	Wet	145	
8-Jan-92	0.58	3.97	716	1053		-	-	1118	Wet	1118	4
Total					3351					3205	
Bias %										-4.4	
		Pacc									
	0.00	0.00									
4-Dec-92	0.30	0.30	74	102		46	-	-	Dry	46	
6-Dec-92	0.13	0.38	74	102		1	-	-	Dry	1	
7-Dec-92	1.77	2.15	393	466		720	-	-	Dry	720	
8-Dec-92	0.73	2.89	505	566		-	-	1205	Wet	1205	
11-Dec-92	0.07	2.87	512	569		-	-	6	Wet	6	
12-Dec-92	0.06	2.93	512	569		-	-	2	Wet	2	1
Total					2139					1980	
Bias %										-7.4	
		Pacc									
	0.00	0.00									
19-Feb-96	0.12	0.12	0	0		-	8	-	Norm	8	
20-Feb-96	1.36	1.48	190	350		-	1132	-	Norm	1132	
21-Feb-96	0.95	2.43	288	543		-	-	1535	Wet	1535	

Date		Pacc								
22-Feb-96	0.14	2.57	288	543	-	-	13	Wet	13	2
Total					3001				2688	
Bias %									-10.4	
		Pacc								
	0.00	0.00								
26-Nov-97	0.46	0.46	81	114	61	-	-	Dry	61	
27-Nov-97	0.23	0.69	101	159	23	-	-	Dry	23	
30-Nov-97	0.22	0.83	138	193	-	32	-	Norm	32	
1-Dec-97	0.26	1.08	175	218	-	33	-	Norm	33	
5-Dec-97	0.39	1.32	245	294	-	100	-	Norm	100	
6-Dec-97	2.55	3.87	896	1313	-	-	13113	Wet	13113	
7-Dec-97	0.11	3.99	896	1314	-	-	8	Wet	8	
8-Dec-97	0.12	4.11	896	1324	-	-	6	Wet	6	3
Total					8399				13375	
Bias %									59.2	
		Pacc								
	0.00	0.00								
29-Jan-98	0.28	0.28	31	52	-	34	-	Norm	34	
30-Jan-98	0.13	0.41	33	52	-	11	-	Norm	11	
1-Feb-98	0.01	0.38	33	52	-	0	-	Norm	0	
2-Feb-98	0.45	0.83	71	93	-	66	-	Norm	66	
3-Feb-98	1.50	2.33	306	437	-	1480	-	Norm	1480	
4-Feb-98	0.57	2.90	316	437	-	-	1036	Wet	1036	
6-Feb-98	0.75	3.61	436	622	-	-	1344	Wet	1344	
7-Feb-98	0.81	4.42	543	730	-	-	1432	Wet	1432	
8-Feb-98	0.94	5.36	680	908	-	-	1796	Wet	1796	
9-Feb-98	0.20	5.56	680	945	-	-	38	Wet	38	4
Total					7402				7236	
Bias %									-2.2	
		Pacc								
	0.00	0.00								
2-Feb-04	0.10	0.10	0	0	-	-	30	Wet	30	

Date		Pacc									
3-Feb-04	0.70	0.81	142	159		-	-	1214	Wet	1214	
4-Feb-04	0.07	0.87	142	159		-	-	1	Wet	1	2
Total					1159					1245	
Bias %										7.5	
		Pacc									
	0.00	0.00									
27-Dec-04	0.21	0.21	14	1		-	12	-	Norm	12	
28-Dec-04	2.30	2.51	464	658		-	5201		Norm	5201	
29-Dec-04	1.57	4.08	957	1648		-	-	6519	Wet	6519	
30-Dec-04	0.16	4.24	957	1650		-	-	62	Wet	62	0
Total					11296	0	5213	6581		11795	
Bias %										4.4	
		Pacc									
	0.00	0.00									
22-Jan-08	0.06	0.06	0	0		-	1	-	Norm	1	
23-Jan-08	0.31	0.37	43	80		-	36	-	Norm	36	
24-Jan-08	0.63	1.00	134	222		-	118	-	Norm	118	
25-Jan-08	1.26	2.26	316	417		-	942	-	Norm	942	
26-Jan-08	0.34	2.60	320	475		-	-	174	Wet	174	
27-Jan-08	1.41	4.02	530	811		-	-	4162	Wet	4162	
28-Jan-08	0.54	4.55	589	865		-	-	513	Wet	513	
29-Jan-08	0.02	4.57	589	865		-	-	0	Wet	0	3
Total					4128					5946	
Bias %										44.1	
		Pacc									
	0.00	0.00									
5-Feb-09	0.25	0.25	62	103		-	-	83	Wet	83	
6-Feb-09	0.58	0.82	150	276		-	-	486	Wet	486	
7-Feb-09	0.38	1.21	229	415		-	-	212	Wet	212	
8-Feb-09	0.09	1.30	244	448		-	-	12	Wet	12	
9-Feb-09	0.27	1.57	282	517		-	-	82	Wet	82	3
13-Feb-09	0.23	1.68	320	561		-	-	32	Wet	32	

Date					Dry	Norm	Wet	Class	Runoff	
16-Feb-09	0.60	2.20	439	680	-	-	627	Wet	627	
17-Feb-09	0.22	2.42	462	726	-	-	35	Wet	35	2
Total				1756					1569.2	
Bias %									-10.6	
		Pacc								
	0.00	0.00								
17-Dec-10	0.14	0.14	0	0	10	-	-	Dry	10	
18-Dec-10	0.36	0.50	36	68	36	-	-	Dry	36	
19-Dec-10	0.99	1.50	175	261	-	606	-	Norm	606	
20-Dec-10	1.50	3.00	429	831	-	-	5310	Wet	5310	
21-Dec-10	0.72	3.73	530	1044	-	-	1009	Wet	1009	
22-Dec-10	1.34	5.06	843	1720	-	-	4481	Wet	4481	
23-Dec-10	0.24	5.30	843	1720	-	-	305	Wet	305	0
Total				13307					11757	
Bias %									-11.6	

Table A 16: Comparison of water volumes calculated based on Landsat images and full model.

Date	Runoff (ac-ft)		Bias (%)
	Landsat	**Full Model**	
Dec-91	3351	3205	-4.5
Dec-92	2139	1980	-7.4
Feb-96	3001	2688	-10.4
Nov-97	8399	13375	59.3
Jan-98	7402	7236	-2.2
Feb-04	1159	1245	7.5
Dec-04	11296	11795	4.4
Jan-08	4128	5946	44.0
Feb-09	1756	1569	-10.6
Dec-10	13307	11757	-11.6